University of Zurich[UZH]

Zurich Open Repository and Archive
University of Zurich
University Library
Strickhofstrasse 39
CH-8057 Zurich
www.zora.uzh.ch

Year: 2011

CAMTA1 is a novel tumour suppressor regulated by miR-9/9(*) in glioblastoma stem cells

Schraivogel, D ; Weinmann, L ; Beier, D ; Tabatabai, G ; Eichner, A ; Zhu, J Y ; Anton, M ; Sixt, M ; Weller, M ; Beier, C P ; Meister, G

Abstract: Cancer stem cells or cancer initiating cells are believed to contribute to cancer recurrence after therapy. MicroRNAs (miRNAs) are short RNA molecules with fundamental roles in gene regulation. The role of miRNAs in cancer stem cells is only poorly understood. Here, we report miRNA expression profiles of glioblastoma stem cell-containing CD133(+) cell populations. We find that miR-9, miR-9(*) (referred to as miR-9/9(*)), miR-17 and miR-106b are highly abundant in CD133(+) cells. Furthermore, inhibition of miR-9/9(*) or miR-17 leads to reduced neurosphere formation and stimulates cell differentiation. Calmodulin-binding transcription activator 1 (CAMTA1) is a putative transcription factor, which induces the expression of the anti-proliferative cardiac hormone natriuretic peptide A (NPPA). We identify CAMTA1 as an miR-9/9(*) and miR-17 target. CAMTA1 expression leads to reduced neurosphere formation and tumour growth in nude mice, suggesting that CAMTA1 can function as tumour suppressor. Consistently, CAMTA1 and NPPA expression correlate with patient survival. Our findings could provide a basis for novel strategies of glioblastoma therapy.

DOI: https://doi.org/10.1038/emboj.2011.301

Posted at the Zurich Open Repository and Archive, University of Zurich
ZORA URL: https://doi.org/10.5167/uzh-50514
Journal Article
Accepted Version

Originally published at:
Schraivogel, D; Weinmann, L; Beier, D; Tabatabai, G; Eichner, A; Zhu, J Y; Anton, M; Sixt, M; Weller, M; Beier, C P; Meister, G (2011). CAMTA1 is a novel tumour suppressor regulated by miR-9/9(*) in glioblastoma stem cells. The EMBO Journal, 30(20):4309-4322.
DOI: https://doi.org/10.1038/emboj.2011.301

CAMTA1 is a novel tumor suppressor regulated by miR-9/9* in glioblastoma stem cells

Daniel Schraivogel[1]#, Lasse Weinmann[2,3]#, Dagmar Beier[4,5], Ghazaleh Tabatabai[6], Alexander Eichner[7], Jia Yun Zhu[2], Martina Anton[8], Michael Sixt[7], Michael Weller[6], Christoph P. Beier[4,5] & Gunter Meister[1,2]*

[1] Biochemistry Center Regensburg (BZR), University of Regensburg, Universitätsstrasse 31, 93053 Regensburg, Germany

[2] Laboratory of RNA Biology, Max-Planck-Institute of Biochemistry, Am Klopferspitz 18, 82152 Martinsried, Germany

[3] present address: Tulbeckstrasse 21, 80339 Munich, Germany

[4] Department of Neurology, RWTH Aachen, Pauwelsstrasse 30, 52074 Aachen, Germany

[5] Department of Neurology, University of Regensburg, Universitätsstraße 84, 93053 Regensburg, Germany

[6] Department of Neurology, University Hospital Zurich, Frauenklinikstrasse 26, CH-8091 Zurich, Switzerland

[7] IST Austria (Institute of Science and Technology Austria), Am Campus 1, 3400 Klosterneuburg, Austria

[8] TU Munich, Institute of experimental oncology and therapy research, Ismaningerstrasse 22, 81675 Munich, Germany

*corresponding author (e-mail: gunter.meister@vkl.uni-regensburg.de; phone: +49 941 943 2847; fax: +49 941 943 2936)

# both authors contributed equally to this work

Abstract

Cancer stem cells or cancer initiating cells are believed to contribute to cancer recurrence after therapy. MicroRNAs (miRNAs) are short RNA molecules with fundamental roles in gene regulation. The role of miRNAs in cancer stem cells is only poorly understood. Here we report miRNA expression profiles of glioblastoma stem cell-containing CD133+ cell populations. We find that miR-9, miR-9* (referred to as miR-9/9*), miR-17 and miR-106b are highly abundant in CD133+ cells. Furthermore, inhibition of miR-9/9* or miR-17 leads to reduced neurosphere formation and stimulates cell differentiation. Calmodulin-binding transcription activator 1 (CAMTA1) is a putative transcription factor, which induces the expression of the anti-proliferative cardiac hormone natriuretic peptide A (NPPA). We identify CAMTA1 as a miR-9/9* and miR-17 target. CAMTA1 expression leads to reduced neurosphere formation and tumor growth in nude mice suggesting that CAMTA1 can function as tumor suppressor. Consistently, CAMTA1 and NPPA expression correlate with patient survival. Our findings could provide a basis for novel strategies of glioblastoma therapy.

Introduction

MiRNAs are fundamental regulators of gene expression that direct processes as diverse as cell metabolism, lineage specification or cell differentiation (Bartel, 2009; Bushati & Cohen, 2007). MiRNAs are small RNA molecules with a size of about 18-25 nucleotides (nt). MiRNA genes are transcribed to primary miRNA transcripts, which are processed to miRNA precursors (pre-miRNAs) by the microprocessor complex in the nucleus. Pre-miRNAs fold into characteristic hairpin structures and are transported into the cytoplasm, where Dicer processes pre-miRNAs and generates a short double stranded RNA. In further steps, one strand directly interacts with a member of the Argonaute (Ago) protein family (Hutvagner & Simard, 2008; Peters & Meister, 2007) and is incorporated into a miRNA-protein complex referred to as miRNP (Carthew & Sontheimer, 2009; Kim et al, 2009; Krol et al, 2010). The other strand, referred to as miRNA* (miRNA star), is degraded. In rare cases, however, both strands can give rise to functional miRNAs. One example for such a bifunctional miRNA is the miR-9/9* pair (Packer et al, 2008). MiRNAs guide miRNPs to partially complementary target sites on mRNAs and the miRNP-mRNA interaction leads to inhibition of translation or mRNA degradation (Huntzinger & Izaurralde, 2011).

MiRNAs are fundamental regulators of basic cellular processes such as cell cycle control, cell differentiation and proliferation (Bartel, 2009; Bushati & Cohen, 2007) and are frequently de-regulated in tumors (Calin & Croce, 2006; Croce, 2009; Esquela-Kerscher & Slack, 2006; Garzon et al, 2009). Numerous miRNA-profiling studies revealed that miRNA expression is altered in almost all types of cancer. Depending on the target mRNAs they regulate, miRNAs can be classified as tumor suppressors or oncogenes. The miRNAs miR-15 and miR-16 (chronic lymphocytic leukemia, CLL), the let-7 family (lung and breast cancer) as well as miR-34 (pancreatic, colon and breast cancer) are well-characterized tumor suppressors (Calin et al, 2002; He et al, 2007; Johnson et al, 2005; Tarasov et al, 2007). On the other hand,

miRNAs such as miR-155 (lymphomas), the miR-17-92 (lymphomas) cluster or miR-21 (variety of different cancers including glioblastomas) have been characterized as oncogenes (Chan et al, 2005; Costinean et al, 2006; He et al, 2005).

Cell populations with stem cell-like properties including self-renewal and differentiation have been identified in a variety of tumors (Lobo et al, 2007). These cancer stem cells (also referred to as tumor initiating cells) can initiate tumor growth, whereas other tumor cells fail to form new tumors when injected into nude mice. Cancer stem cells can be enriched in cell fractions that express specific surface proteins, such as CD44 in breast cancer or CD133 in colorectal cancer and a subgroup of primary astrocytic glioblastoma (Gilbertson & Rich, 2007; Lobo et al, 2007; Visvader & Lindeman, 2008; Tabatabai & Weller, 2011). According to the cancer stem cell hypothesis, cancer stem cells are believed to be the cause of relapse after therapy and contribute to teatment resistance (Reya et al, 2001). MiRNA expression profiling has been performed in several different tumor stem cell populations. In breast cancer cells, for example, it has been shown that let-7 regulates self-renewal and tumorigenicity of cancer initiating cells (Yu et al, 2007). Moreover, miR-34a is required for prostate cancer stem cell function and inhibition of miR-34a leads to reduced tumor growth (Liu et al, 2011). A detailed characterization of miRNA expression in glioblastoma stem cells has not yet been performed.

Here we report the miRNA expression profile of $CD133^+$ glioblastoma cell populations. We find that miR-9, miR-9*, miR-106b and miR-17 are highly abundant in glioblastoma stem cells. We further find that inhibition of miR-9/9* promotes neuronal differentiation suggesting that miR-9/9* inhibit differentiation of glioblastoma stem cells and maintain their stemness. We identify the calmodulin-binding transcription activator 1 (CAMTA1) as miR-9/9* target. CAMTA1 over-expression substantially reduces colony formation, demonstrating that CAMTA1 is a novel tumor suppressor in glioblastoma. Consistently, we find that CAMTA1 expression correlates with glioblastoma patient survival. CAMTA1 is a putative

transcription factor and we show that CAMTA1 regulates the expression of the natriuretic peptide A (NPPA, also referred to as atrial natriuretic factor (ANF)), which gives rise to peptide hormones with anti-proliferative effects.

Results

miRNA expression profiling of CD133$^+$ glioblastoma stem cells

In order to analyze the contribution of miRNAs to the biology of glioblastoma stem cells, we isolated stem cell-containing CD133$^+$ cells from the primary glioblastoma cell line R11 (Beier et al, 2007; Beier et al, 2008) by fluorescence-activated cell sorting (FACS, Figure 1A and 1B). Total RNA was extracted from CD133$^+$ and CD133$^-$ cells and small RNA libraries were generated and sequenced (Figure 1C and suppl. Table 1 and 2). A detailed analysis of the individual miRNAs revealed that miR-9*, miR-17-5p, miR-106b and miR-15b were highly abundant in CD133$^+$ cells, whereas miR-221, miR-222, miR-27a and miR-21 were more specific to CD133$^-$ cells (Figure 1D). The sequencing data were further validated by Northern blotting. Signals for miR-17-5p, miR-9*, miR-106b and also miR-9 were much stronger in CD133$^+$ cells (Figure 1E) demonstrating that these miRNAs are indeed differentially expressed between CD133$^+$ and CD133$^-$ cells. Since the miR-9/9* pair was highly abundant in CD133$^+$ R11 cells, we next confirmed the differential miR-9/9* expression in CD133$^+$ cells in additional primary glioblastoma cell lines by qPCR (Beier et al, 2007) (Figure 1F). Consistent with the data obtained from R11 cells, miR-9/9* expression is increased in CD133$^+$ cell populations of many glioblastoma cell lines, whereas miR-34a was either not changed or less abundant in CD133$^+$ cells. Although miR-9/9* expression is always stronger in CD133+ cells (with the exception of miR-9* in R54 cells, middle panel), some cell lines show only mild differences in miR-9/9* expression in CD133+ cells compared CD133- cells. This might be due to the different tumor origin of the cell lines.

miR-9/9* are required for neurosphere formation and glioblastoma stem cell maintenance

$CD133^+$ glioblastoma cell populations show a neurosphere-like growth in tissue culture based colony formation assays. Therefore, we analyzed the impact of $CD133^+$-specific miRNAs on neurosphere formation. Primary glioblastoma cells were transfected with 2'-O-methylated antisense inhibitors against miR-9, miR-9*, miR-17-5p or miR-106b and neurosphere growth was analyzed (Figure 2A and suppl. Figure 1 for validation of miRNA inhibition). Inhibition of miR-9 as well as miR-9* led to strongly reduced neurosphere formation. Inhibition of miR-17-5p reduced colony formation significantly whereas miR-106b inhibition had no effect (Figure 2A). Conversely, transfection of a miR-9/9* mimic increased neurosphere formation of primary glioblastoma cells (Figure 2B).

Since both inhibition of miR-9/9* and miR-17-5p affected neurosphere formation, we analyzed whether the simultaneous inhibition of two miRNAs caused additive effects (Figure 2C). Indeed, the effects of miR-9 or miR-9* inhibition were significantly stronger, when miR-17-5p was co-inhibited, suggesting that both miRNAs function independently of each other and contribute to neurosphere formation. Of note, much lower inhibitor concentrations were used for the double-inhibition experiments and therefore the overall numbers differ from the experiments shown in Figure 1A.

Because miR-9/9* are highly abundant in $CD133^+$ cells we asked if inhibition of these miRNAs may influence the $CD133^+$ cell population. Primary glioblastoma cells were transfected with inhibitors against miR-9 or miR-9* and $CD133^+$ cells were sorted (Figure 2D). Indeed, inhibition of miR-9 or miR-9* led to a reduction of the $CD133^+$ cell population, suggesting that both miRNAs are required for $CD133^+$ glioblastoma stem cell maintenance. Reduced stem cell maintenance might lead to increased cell differentiation of primary glioblastoma cells. Thus, miR-9 or miR-9* was blocked and the neuronal differentiation marker Tuj1 or the glial marker GFAP were analyzed by Western blotting. Strikingly,

$CD133^+$ cell-depleted populations exhibited induced neuronal differentiation as evident from increased Tuj1 expression, whereas glial differentiation appeared not to be affected by miR-9/9* inhibition (Figure 2E). In summary, our data suggest that miR-9/9* help maintaining $CD133^+$ cells probably by preventing differentiation.

$CD133^+$ cancer stem cell miRNAs regulate the putative transcription factor CAMTA1

In order to understand the role of miR-9/9* in glioblastoma stem cells, it is important to know the identity of their individual target mRNAs. To find miR-9* targets in primary glioblastoma cells, we transfected inhibitors against miR-9* or control inhibitors and immunoprecipitated Ago2-bound mRNAs (Figure 3A) (Beitzinger et al, 2007; Easow et al, 2007; Karginov et al, 2007). The miRNA inhibitor prevents mRNA binding and therefore miR-9* targets are selectively lost in the immunoprecipitates compared to control transfections. Using this approach, we identified a number of mRNAs that are strongly reduced in anti-Ago2 immunoprecipitates when miR-9* was inhibited (Figure 3B). We focused on CAMTA1, because it is expressed from the 1p36 locus that is frequently deleted in a subset of gliomas (Finkler et al, 2007). Strikingly, a minimal deletion comprising only the CAMTA1 gene has been identified, suggesting that CAMTA1 is indeed important for glioma formation (Barbashina et al, 2005).

We found that the CAMTA1 3' untranslated region (UTR) not only contains binding sites for miR-9* but also for miR-9, miR-106b and miR-17-5p, which are also highly abundant in $CD133^+$ cell populations (Figure 4A). The CAMTA1 3' UTR was fused to firefly luciferase and co-transfected together with inhibitors against miR-9/9* (Figure 4B, panels 1 and 2), miR-106b (panel 3) or miR-17-5p (panel 3) into primary glioblastoma cells. In all cases, firefly expression was elevated upon miRNA inhibition. Increased firefly activity was not observed, when reporters with mutated miR-9 or miR-9* binding sites were transfected. Furthermore, endogenous CAMTA1 mRNA as well as protein levels were elevated, when

miR-9 or miR-9* was inhibited (Figure 4C and D). Of note, protein levels were much stronger increased than mRNA levels suggesting that miR-9/9* may preferentially inhibit CAMTA1 translation. Since miR-9 and miR-9* inhibition blocked neurosphere formation, we hypothesized that this effect could be mediated through the induction of CAMTA1. Therefore, CAMTA1 was depleted by RNAi in primary glioblastoma cells (suppl. Figure 2) and after 2 days, miR-9 or miR-9* was inactivated with antisense oligonucleotides (Figure 4E). Indeed, miR-9 inhibition effects on colony formation were rescued by CAMTA1 depletion. We also observed a significant rescue of miR-9* inhibition, although not as strong as observed for miR-9.

CAMTA1 functions as tumor suppressor in glioblastoma cells

It has been suggested that CAMTA1 functions as tumor suppressor in neuroblastoma (Finkler et al, 2007; Henrich et al, 2011). However, a link between CAMTA1 function and glioblastoma has not been reported so far. To address this question, we cloned the CAMTA1 cDNA and transfected it into primary glioblastoma cells (Figure 5A, B and C). Strikingly, over-expression of CAMTA1 let to strongly reduced neurosphere formation both in R11 and R28 cells. CAMTA1 is a putative transcription factor that contains a N-terminal DNA binding domain (Figure 5A). We deleted the DNA binding domain (Figure 5D), transfected the mutated CAMTA1 into primary glioblastoma cells and again analyzed neurosphere formation. Interestingly, the ΔN mutant that cannot bind DNA has no inhibitory effect on colony formation, indicating that over-expression of functional CAMTA1 inhibits neurosphere formation. Since miR-9/9* negatively regulate CAMTA expression, we hypothesized that CAMTA1 over-expression should have a similar effect on the $CD133^+$ cell compartment as miR-9/9* inhibition (see Figure 2B). Indeed, over-expression of CAMTA1 reduced the number of $CD133^+$ cells suggesting that the miR-9/9* effect is at least in part due to CAMTA1 inhibition (Figure 5E).

To further analyze the observed tumor suppressor activity of CAMTA1 in vivo, a R28 cell line stably expressing luciferase was transfected either with an empty plasmid or with a plasmid containing wild type (wt) CAMTA1 (Figure 6). After transfection, cells were injected into nude mice and tumor growth was analyzed 15 days after transfection by measuring luciferase activity. In agreement with the in vitro data, cells transfected with wt CAMTA1 showed strongly decreased tumor growth, whereas control cells formed tumors rapidly (Figure 6A and 6B). In summary, we have shown that CAMTA1 functions as tumor suppressor both in vitro and in vivo.

The striking effect of CAMTA1 over-expression on colony formation and tumor growth prompted us to ask whether CAMTA1 expression also correlates with survival of patients suffering from astrocytoma or glioblastoma. We analyzed mRNA expression data sets from large patient cohorts using the Repository of Molecular Brain Neoplasia Data (REMBRANDT) and The Cancer Genome Atlas (TCGA) (Figure 7A and B). CAMTA1 mRNA expression was strongly decreased in astrocytoma as well as glioblastoma patients compared to healthy individuals. Notably, grade IV glioblastomas show lower CAMTA1 expression than the less malignant astrocytomas. These results are in line with our previous results indicating a significant down-regulation of CAMTA1 mRNA in cancer stem cells compared to neural stem cells (Lottaz et al, 2010). Finally, we correlated glioblastoma patient survival with low or intermediate (blue) and high (red) CAMTA1 expression (Figure 7C). Strikingly, glioblastoma patients with high CAMTA1 levels survived much longer than patients with lower or intermediate CAMTA1 expression indicating that CAMTA1 is a tumor suppressor with a high prognostic value.

CAMTA1 stimulates the expression of the anti-proliferative peptide NPPA

It has been shown that CAMTA2, which is highly homologous to CAMTA1, activates transcription of the natriuretic peptide A (NPPA) in the heart (Song et al, 2006). Interestingly,

it has been demonstrated that NPPA has an anti-proliferative effect on glioblastoma cells in vitro (Vesely et al, 2007). We analyzed whether CAMTA1 also activates the expression of NPPA in glioblastoma cells. A plasmid expressing wt CAMTA1 or a mutant lacking the DNA-binding domain was transfected into LNT-229 cells and NPPA expression was analyzed by qPCR (Figure 8A). Wild-type CAMTA1 expression led to an increase of NPPA expression, while transfection of the mutated CAMTA1 had a much weaker effect. NPPA is a short secreted peptide, which is taken up by the natriuretic peptide receptor A (NPR-A). Therefore, we tested NPR-A expression and found that the receptor for NPPA is upregulated by CAMTA1 expression as well (Figure 8B). Finally, since miR-9, miR-9* and miR-17 regulate CAMTA1 expression in CD133+ cells, we tested whether inhibition of these miRNAs induces NPPA or NPR-A expression. MiRNAs were inhibited using 2'-O-methylated inhibitors and NPPA or NPR-A expression was subsequently analyzed by qPCR (Figure 8C). Strikingly, inhibition of miR-9/9* or miR-17 increased NPPA and NPR-A expression presumably by inducing CAMTA1 expression.

NPPA has a strong anti-proliferative effect on glioblastoma cells in vitro and therefore we analyzed whether NPPA expression correlates with patient survival (Figure 7D). We used the REMBRANDT database for our investigations. Consistent with our experimental data, we found that expression of NPPA correlates with patient survival. Patients with high NPPA levels (red) survived much longer than patients with intermediate (blue) and low (green) NPPA levels.

Taken together, we have found that miR-9/9* and miR-17 regulate the expression of the novel tumor suppressor CAMTA1 in $CD133^+$ glioblastoma cells and CAMTA1 itself stimulates the expression of the anti-proliferative peptide NPPA.

Discussion

MiRNAs have been implicated in almost all types of cancer (Calin & Croce, 2006; Esquela-Kerscher & Slack, 2006; Garzon et al, 2009). However, only a few studies have analyzed the function of miRNAs in cancer stem cells (Ji et al, 2009; Shimono et al, 2009; Wong et al; Yu et al, 2007). We found that miR-9 and its corresponding miR-9* are highly expressed in cancer stem cell populations obtained from a subgroup of primary astrocytic glioblastomas. Both miRNAs function as oncogenes by repressing the novel tumor suppressor CAMTA1. Consistently, it has been shown that miR-9/9* are highly expressed in primary brain tumors (Huse et al, 2009; Nass et al, 2009). A recent study has analyzed miRNA expression in 261 glioblastoma samples (Kim et al, 2011). According to their miRNA and mRNA expression profiles, glioblastomas were separated into five classes: glioblastomas with neural precursors, with oligoneural precursors, with multipotent precursors, with astrocytic precursors and with neuromesenchymal precursors. Interestingly, miR-9/9*, miR-17 or miR-106 were only found in glioblastomas with oligoneural precursors (Kim et al, 2011). It is thus unlikely that miR-9/9* or miR-17 inhibition would affect all glioblastomas. It is more likely that only those tumors with oligoneural precursors are affected. These findings have also impact on possible therapeutic approaches. Glioblastomas need to be classified by miRNA expression profiling first before miRNA inhibition could be used as potential treatment. However, it is important to note that glioblastomas have been classified using various approaches and the obtained classes very often differ significantly (Huse et al, 2011; Lottaz et al, 2010; Phillips et al, 2006; Verhaak et al, 2010).

MiR-9 has been implicated in cancer before. It is involved in cancer metastasis in breast cancer cells (Ma et al, 2010) or in colorectal cancer (Zhu et al, 2011). Interestingly, miR-9 expression is stimulated by MYCN in breast cancer and MYCN is closely related to the frequent 1p36 deletion (Ma et al, 2010; Mestdagh et al, 2010). It is tempting to speculate that MYCN might contribute to miR-9/9* expression in glioblastoma as well. Very recently, it has been demonstrated that among others, expression levels of miR-9 and miR-17 are correlated

with malignant progression of gliomas (Malzkorn et al, 2010). In addition, miR-9 has been implicated in oligodendroglioma (Nelson et al, 2006). This supports our finding that these miRNAs are important for glioma pathogenesis. Furthermore, miR-9 is also important for neural development, neuronal stem cell fate determination and for proliferation and migration of neural progenitors (Delaloy et al, 2010; Yoo et al, 2009; Zhao et al, 2009) supporting our model that miR-9 is important for glioblastoma stem cell function. Our data provide evidence that the bi-functional miR-9/9* inhibits CAMTA1 expression in glioblastoma stem cells and thereby contributes to robust cancer stem cell survival. We have demonstrated that expression of CAMTA1 in glioblastoma cells causes a strong reduction of colony formation both in vitro and in a xenograft model system. Therefore, we suggest that CAMTA1 is a novel tumor suppressor gene functioning in glioblastoma. Strikingly, it has been shown very recently that CAMTA1 has tumor suppressor activity in neuroblastoma cells supporting the idea that CAMTA1 is a tumor suppressor in a larger variety of neural tumors (Henrich et al, 2011).

The molecular functions of CAMTA1 have not been studied in detail yet. It has been shown in flies that CAMTA functions as transcription activator and is involved in the function of Rhodopsin, a G protein coupled light receptor (Han et al, 2006). In mammals, at least two CAMTA genes exist. The loss of CAMTA2 promotes cardiomyocyte hypertrophy (Song et al, 2006). Since CAMTA proteins can activate the expression of NPPA in the heart, we asked whether NPPA might also play a role in glioblastoma. Indeed, it has been demonstrated that NPPA, when incubated with glioblastoma and also other cancer cells, has a strong anti-proliferative effect in vitro (Vesely et al, 2007; Vesely et al, 2005). Strikingly, CAMTA1 activates NPPA expression in glioblastoma cells as well. Moreover, CAMTA1 also stimulates the expression of the NPPA receptor, which might explain the tumor suppressor function of CAMTA1. Additionally, the NPPA gene is located in the 1p36 locus, and it is indeed deleted in a number of glioma (Ichimura et al, 2008).

Based on our data, we propose the following model. In $CD133^+$ cells miR-9/9* and miR-17 expression is high compared to $CD133^-$ cells, which results in low CAMTA1 expression. Of note, it is likely these miRNAs regulate several other target mRNAs, which might contribute to the observed phenotype as well. CAMTA1 inhibition also represses the expression of the secreted peptide NPPA. Upon CAMTA1 activation, NPPA expression is induced and the peptide is secreted. In parallel, CAMTA1 also stimulates the expression of the NPPA receptor NPR-A in order to allow cells to respond to NPPA. Since CAMTA1 expression is particularly low in the $CD133^+$ fraction of many of our analyzed glioblastoma cell lines (suppl. Figure 3), it is tempting to speculate that the expression and also the sensitivity to the anti-proliferative peptide NPPA is repressed by miR-9/9* and miR-17 regulation of CAMTA1.

Further analysis of the cellular functions of the tumor suppressor CAMTA1 as well as its regulators miR-9/9* may finally lead to a better understanding of glioblastoma pathogenesis and ultimately to more efficient therapies that might be based on miR-9 and miR-9* inhibitors.

Materials and Methods

Isolation of Ago2-associated RNAs

R11 cells were reverse transfected in four 10 cm plates per sample with miR-122 (control) or miR-9* 2'-O-methylated antisense oligonucleotide inhibitors for 2d. Cells were lysed in 500 µl lysis buffer (150 mM KCl/25 mM Tris-HCl pH 7.5/2 mM EDTA/1mM NaF/0.5% NP-40/0.5 mM DTT/0.5 mM AEBSF) per plate. Ribolock (Fermentas, 1µl per ml of lysis buffer) was added before lysis. Lysates were cleared by centrifugation at 16000 g for 10 min. For immunoprecipitation (IP) of endogenous Ago2, 3 ml of monoclonal anti-Ago2 11A9 hybridoma supernatant was coupled to 100 µl protein G-Sepharose (GE Healthcare) for 10 h at 4°C. Coupled beads were washed twice with PBS and subsequently incubated with cell lysate for 4 h at 4°C. All IP samples were washed three times with IP wash buffer (300 mM

NaCl/50 mM Tris pH 7.5/1mM NaF, 0.01% NP-40/5 mM $MgCl_2$) and once with PBS. IP samples and corresponding samples containing 10% of input lysate were proteinase K-digested, followed by phenol/chloroform/isopropyl alcohol extraction and precipitation of RNA in 80% ethanol at -20°C. RNA was pelleted, dried and treated with DNaseI (Fermentas) for 45 min at 37°C, followed by thermal inactivation of DNaseI. RNA integrity was assessed via Agilent 2100 Bioanalyzer (Agilent Technologies) prior to microarray hybridization.

Microarray experiments and data analysis

RNA from anti-Ago2 IP and input samples was processed using the SuperAmp RNA amplification protocol (Miltenyi Biotec). cDNA integrity was checked via Bioanalyzer platform. 250 ng of each cDNA was labeled with Cy3 dye (Miltenyi Biotec) according to the manufacturer's protocol. Samples were hybridized to Agilent Whole Human Genome 4x44 K Oligo Microarrays. Fluorescence signals of the hybridized Agilent Microarrays were detected using Microarray Scanner System (Agilent Technologies).

Microarray data were analyzed using Agilent Genespring software. Expression values below 0.01 were set to 0.01. Each measurement was divided by the 50th percentile of all measurements in that sample. All IP samples were normalized to the corresponding input RNA samples: The IP sample from control antagomir-transfected cells was normalized against the median of the corresponding input RNA sample and the IP sample from miR-9* antagomir-transfected cells was normalized against the median of the corresponding input RNA sample. For normalization, each measurement for each gene in the IP samples was divided by the median of that gene's measurements in the corresponding input RNA samples. IP to input ratios from miR-9* transfected samples were then devided by the IP to input ratios from control transfected sample.

Using this normalization procedure, the normalized expression value of each transcript in IP samples directly reflects its fold enrichment in the immunoprecipitated transcript pool relative

to the input RNA pool. To filter for potential miRNA target mRNAs bound by Ago2, all transcripts that were >5-fold enriched in IPs from control antagomir-transfected cells were identified. Transcripts where the enrichment in miR-9* antagomir-transfected cells was >10-fold lower than in control-transfected cells were considered to be potential targets of miR-9*.

Cell culture and transfection

R11, R20, R28, R40, R44, and R52 cells were cultured at 37°C in DMEM-F12 medium supplemented with 20 ng/mL of each human recombinant epidermal growth factor, human recombinant basic fibroblast growth factor (both from R&D Systems), and human leukemia inhibitory factor (Millipore), 2% B27 supplement (Invitrogen), 1% penicillin/streptomycin solution (PAA), and 1% MEM vitamins solution (Invitrogen). Cells were passaged every 7-10 days by trypsinization or by detaching with a pipette. 50% of the medium was substituted twice weekly. HEK 293T, T98G and LNT-229 cells were cultured in DMEM supplemented with 10% fetal bovine serum and 1% penicillin/streptomycin solution. Typically, cells were passaged every 3 days by trypsinization in a 1:10 ratio.

R11 cells ($1x10^5$ cells per well) were reverse transfected with 100 nM 2'-O-methyl oligonucleotides or 40 nM siRNAs in 6 well plates with 5 μL/well Lipofectamine 2000 (Invitrogen). For cotransfection of two 2'-O-methyl antisense oligonucleotides, each oligo was added to 50 nM final concentration, to give an overall concentration of 100 nM. The transfection mix was removed 24 h post transfection, and fresh medium was added. T98G cells were transfected with Lipofectamine 2000 12 h after seeding according to the manufacturer's instructions, using 40 nM siRNAs or 80 nM 2'-O-methyl oligonucleotides.

For plasmid transfections, R11, R28 and R28-luc cells were electroporated using the Nucleofector Kit for mouse neural stem cells (Lonza), according to the manufacturer's instructions and the Nucleofector Device II (Lonza). In short, cells were detached by pipetting, washed once with DMEM/F12 and $3x10^6$ cells were transfected with 5 ug of

plasmid DNA using Program A-033. Directly after electroporation, cells were transferred into one well of a 6-well plate. Medium was replaced 24 h post transfection. For electroporation of LNT-229 , the cell line nucleofector Kit R (Lonza) was used as described above.

Western Blotting and Northern Blotting

To analyze levels of proteins other than CAMTA1, cells were lysed as previously described (Weinmann et al, 2009). For the analysis of CAMTA1 protein levels or corresponding loading controls, cells were lysed in nuclear lysis buffer (1% SDS, 10 mM EDTA, 50 mM Tris pH 8, 0.1 % sodium deoxycholate, 2 mM 4-(2-Aminoethyl) benzenesulfonyl fluoride hydrochloride, 5 units/ml DNAaseI (Fermentas)) for 20 min and sonicated for 10s on a Bandelin Sonopuls HD2070 sonifier. Lysates were cleared by centrifugation. Western Blotting was performed as previously described (Hock et al, 2007). The following antibodies (dilutions) were used: Anti-mouse-HRP (1:5000), anti-rabbit-HRP (1:5000), mouse-anti-β-Actin AC15 (1:10000), mouse-anti-Tuj1 (1:1000), rabbit-anti-GFAP (1:2000), rabbit-anti-CAMTA1 (1:200). Northern blotting was performed as previously described (Lagos-Quintana et al, 2001) using either 2'-O-methyl oligonucleotide or DNA probes antisense to the miRNA of interest. The sequence of Ile tRNA probe was 5'-TGCTCCAGGTGAGGATCGAAC.

Clonogenicity assays

$1x10^5$ R11 cells were transfected in 6-well plates as indicated. 2'-O-methylated antisense oligonucleotides and synthetic miRNAs were transfected twice with an interval of 7d. 7d after second transfection, cells were counted and approximately 1000 cells were transferred into each well of a 48-well plate. Neurosphere-like clones were counted 4 weeks after plating. The number of clones per well were summed up for each sample and normalized to the number of clones obtained for control-transfected samples. Results of the described clonogenicity assays were reproduced by limited dilution assays with 1 cell per well. Herefore, $1x10^5$ cells were

transfected as indicated above. 7d after second transfection, 1 cell was seeded into each well of a 96-well plate and neurosphere-like clones were counted 4 weeks after plating. Data for limited dilution assays are not shown.

In vivo tumor model and bioluminescence imaging

Intracranial glioblastoma xenografts were established in 10 week old male NMRI:nu/nu mice (Charles River) as described previously (Beier et al, 2007). In brief, tumor cells were treated as indicated. 3 h after transfection, 1.4 x 10^5 viable cells (as determined by trypan blue exclusion) were injected 2mm lateral to the midline and 4mm anterior to bregma to a depth of 3mm using a Hamilton syringe. The bioluminescence of implanted tumor cells was determined 15 d after implantation. 1 min after injection of 150 mg/kg D-luciferin (Biosynth) mice were anesthetized and emitted photons were registered for 5 min using Xenogen IVIS Lumina Imaging System (Caliper Life Sciences). The signal was normalized to background signal. Mice without detectable tumors were excluded from the analysis.

Lentiviral transduction of R28 cells

Glioblastoma stem cells were stably transduced using a lentiviral vector expressing firefly luciferase under control of the constitutive spleen focus forming virus LTR promoter.

Third generation packaging, VSV-pseudotyped, self-inactivating lentiviral vectors were produced by transient transfection of HEK 293T cells using standard protocols (Wubbenhorst et al, 2010). Medium was changed to stem cell medium after 24 h. Supernatants were filtered through 0.45 µm filter and used for spin infection (Leisegang et al, 2008). Individual wells of a 24-well plate were coated with 400 µl RetroNectin (Takara Bio Europe SAS; final concentration 12.5 µg/ml) for two hours at room temperature, subsequently incubated for 30 min. at 37°C with bovine serum albumine (2 % in PBS) and washed with PBS prior to addition of cells. 1×10^5 cells/ml suspension cells were added onto RetroNectin coated wells.

One ml virus containing supernatant supplemented with protamine sulfate (final concentration 4 µg/ml) was added to each well and infection was enhanced by 90 min centrifugation at 32°C and 800 × g. Cells were incubated at 37°C. The next day, cells were washed off the wells, spun, resuspended in 5 ml fresh complete medium and further cultivated.

Cell lines

The generation of R11, R20, R28, R40, R44, and R52 cell lines from glioblastoma samples was previously described (Beier et al, 2007).

Antibodies

The following antibodies were used: Rat-anti-hsAgo2 (11A9, (Rudel et al, 2008)), mouse-anti-Tuj1 MMS-435p (Covance), mouse-anti-β-Actin AC15 (Abcam), rabbit-anti-GFAP (DAKO), anti-CD133-2 293C3-PE (Miltenyi), anti-rabbit-HRP, anti-mouse-HRP (both from Sigma). The polyclonal antibody to CAMTA1 was generated as follows: A GST-tagged fragment containing aa 294-864 of CAMTA1 was expressed in *E. coli* and used for the immunization of rabbits. Polyclonal antiserum was purified and used for western blotting.

Oligonucleotides

2'-O-methyl antisense oligonucleotides and siRNAs/miRNAs were chemically synthesized using RNA phosphoramidites (Pierce) on an Äkta Oligopilot 10 DNA/RNA synthesizer (GE Healthcare), according to the manufacturer's protocol. The sequences of 2'-O-methyl oligonucleotides were miR-9* antisense, 5'-ACUUUCGGUUAUCUAGCUUUAT; miR-17-5p antisense, 5'- ACUACCUGCACUGUAAGCACUUUGT; miR-106b antisense, 5'-AUCUGCACUGUCAGCACUUUAT; miR-9 antisense, 5'-UCAUACAGCUAGAUAACCAAAGAT; miR-122 antisense, 5'-ACAAACACCAUUGUCACACUCCAT; miR-301 antisense, 5'-

GCUUUGACAAUACUAUUGCACUGT; miR-330 antisense, 5'-GCCUAAGACACAGGCCCAGAGAT. The siRNA sequences (sense, antisense) were CAMTA1 siRNA 1, 5'-CTACCGAAGTTATAAGAAAUT, 5'-TTTCTTATAACTTCGGTAGUT; CAMTA1 siRNA 2, 5'-GAAUCAAGCAGGAGAAUUUUT, 5'-AAAUUCUCCUGCUUGAUUCGT; control siRNA 1, 5'-UUGUCUUGCAUUCGACUAAUT, 5'-UUAGUCGAAUGCAAGACAAUT; control siRNA 2, 5'-UCGAAGUAUUCCGCGUACGUT, 5'-CGUACGCGGAAUACUUCGAUT. The sequences of synthetic miRNAs were miR-9, 5'-UCUUUGGUUAUCUAGCUGUAUGAT; miR-9*, 5'-AUAAAGCUAGAUAACCGAAAGUT; miR-122, 5'-UGGAGUGUGACAAUGGUGUUUGT, miR-122*, AACGCCAUUAUCACACUAAAUAT.

Flow cytometry

Cells were trypsinized and washed with DMEM-F12 and FACS buffer (PBS containing 1% BSA). 10^7 cells were resuspended in 80 μL FACS buffer containing 10% FcR blocking reagent (Miltenyi) and incubated for 5 min on ice. 10 μL Anti-CD133-PE was added, and cells were incubated for 10 min on ice in the dark. Cells were pelleted and washed once with FACS buffer. Stained cells were sorted on a FACS Aria system (Becton Dickinson). Cell debris were gated out using a forward scatter/sideward scatter dot plot. CD133-negative and -positive cell populations were identified using unstained cells as control.

RNA isolation

Total RNA for mRNA analyses was isolated using the Prep Ease kit (USB), according to the manufacturer's instructions. For small RNA detection, RNA was isolated using Trifast (Peqlab).

cDNA synthesis

cDNA for mRNA analysis was synthesized with random hexamer primers from 2 μg of total RNA using the First Strand cDNA synthesis kit (Fermentas), according to the manufacturer's protocol. To quantify miRNAs, RNA samples were treated with DNaseI (Fermentas), poly(A)-tailed using the poly(A)-tailing kit (Ambion) and reverse transcribed using the First Strand cDNA synthesis kit and the URT primer AACGAGACGACGACAGACTTTTTTTTTTTTTTV (Hurteau et al, 2006).

qPCR

qPCR was performed on a MyiQ cycler (BioRad) using the Mesa Green qPCR mastermix (Eurogentec). The primers were: GAPDH, 5'-TGGTATCGTGGAAGGACTCATGAC, 5'-ATGCCAGTGAGCTTCCCGTTCAGC; β-Actin, 5'-CTGGAGAAGAGCTACGAGCTG, 5'-TTGAAGGTAGTTTCGTGGATG; CAMTA1, 5'-ATCCTTATCCAGAGCAAATTCC, 5'-AGTTTCTGTTGTACAATCACAG; NPPA, 5'-CAGGATGGACAGGATTGGA, 5'-TCTTCAGTACCGGAAGCTGTT; NPR-A 5'-TCGAAACCACCAAACTCCTC, 5'-AGTGGTGGGACTGAAGATGC; hsa-miR-9, 5'-TCTTTGGTTATCTAGCTGTATG; hsa-miR-9*, 5'-ATAAAGCTAGATAACCGAAAG; hsa-miR-34a; 5'-TGGCAGTGTCTTAGCTGGTTG; U6 snRNA, 5'-GATGACACGCAAATTCGTGAAG; Universal RT primer for miRNA and U6 snRNA detection, 5'-AACGAGACGACGACAGACTTT. Data were evaluated using the ddCt method with GAPDH or β-Actin as reference mRNAs. Error bars were obtained from triplicate PCR samples by propagating the ddCt standard error of the mean through the exponential term as previously described (Livak & Schmittgen, 2001).

Generation and sequencing of small RNA libraries

Small RNA libraries were generated by Vertis Biotechnology AG and sequenced by 454 pyrosequencing as previously described (Tarasov et al, 2007).

Analysis of the sequencing results

Known miRNAs were identified by comparing the sequencing results with annotated miRNAs from the *H. sapiens* miRNA database (miRBase) using the Microsoft Excel software. Several miRNA reads were found to contain sequencing errors, typically starting from nucleotide 18-25 that were possibly due to the procedure of library preparation and/or pyrosequencing. Most errors were poly(A) insertions at the 3'-end of the reads. Therefore, those reads that were fully complementary to a known miRNA from nucleotide 1-18 but had additional A insertions at the 3'-end were re-annotated as miRNAs.

Read numbers for each miRNA were normalized to the total number of reads of the corresponding library. For calculation of miRNA expression, the normalized reads numbers from the CD133-negative cell library were divided by the normalized read numbers from the CD133-negative library.

Luciferase assays

To investigate miRNA effects on reporter constructs, T98G were used for high transfection efficiency and high firefly and renilla expression levels. T98G cells were co-transfected with 2'-O-methylated antisense oligonucleotides (80 nM final concentration) and pMIR-RL constructs (100 ng per well) in 48-well plates, using Lipofectamine 2000. 24 h after transfection, cells were lysed in passive lysis buffer (Promega). Luciferase activities were measured on a Mithras LB 940 luminometer (Berthold technologies). Luciferase substrate reagents were purchased from PJK cryosystems. All samples were assayed in 4 to 6 replicates. Firefly/renilla luminescence ratios for individual samples were normalized to

corresponding ratios of the empty pMIR-RL plasmid and control inhibitor transfected samples.

Plasmids

The pMIR-RL dual luciferase vector was previously described (Beitzinger et al, 2007). The 3'-UTR of CAMTA1 mRNA was PCR-amplified from R28 genomic DNA using the primers 5'-ATACGAGCTCAGACATACAGCAGCATCCCTTAGCAATGTG (forward), 5'-ATACGCCGGCGGAAATTTTCTTCATTTTTAATTTACAGCAG (reverse), digested with SacI and NaeI and ligated into pMIR-RL. For the analysis of miR-9 and miR-9* binding sites, all sites predicted by TargetScan 5.0 and all seed matches that are conserved in mammals and indicated in Fig. 3A were mutated by PCR-based mutagenesis as follows: The nucleotides CAAA in miR-9* seed matches were replaced by GTTT, and the nucleotides CTTT in miR-9* seed matches were replaced by GAAA. A cDNA fragment encoding CAMTA1 was PCR-amplified from Marathon whole human brain cDNA library (BD Bioscience). CAMTA1 orf was re-amplified by using the primers 5'-ATACGATATCATGTGGCGCGCGGAGGGGAAATG (forward) and 5'-ATATGCGGCCGCTCAAGTTCCTTGGCCTTTTTCAATTCTTTCACTC (reverse) bearing EcoRV and NotI restriction sites, respectively, followed by restriction digestion and ligation into pIRESneo. Note that all CAMTA1 clones that were obtained contained an additional exon of 21 nt in size (AGCTGACATGGATAGCCTTGA, data not shown) compared to the Refseq sequence (NM_015215.1). The additional nucleotides are inserted after nt 4687 of NM_015215.1 and encode for 7 additional amino acids which localize to the predicted Calmodulin binding domain. An N-terminal CAMTA1 deletion mutant lacking the amino acids 1-188 (nt 1-564) was cloned into pIRESneo and used as a control. All constructs were verified by sequencing.

Analysis of gene expression in glioma patients and correlation with survival

The results published here are in part based upon data generated by the Repository of Molecular Brain Neoplasia Data (Rembrandt), a project led by the National Cancer Institute (NCI) (The Cancer Genome Atlas, 2008; Madhavan et al, 2009). Information about the Rembrandt Database can be found at https://caintegrator.nci.nih.gov/rembrandt/. TCGA project is a joined effort of the NCI and the National Human Genome Research Institute (NHGRI) (The Cancer Genome Atlas, 2008). Information about TCGA can be found at http://cancergenome.nih.gov.

Statistical analysis

Experiments were performed in three biological replicates, unless stated otherwise. Mean values and standard error of the mean (SEM) were calculated from all biological replicates. Error bars display +/- SEM. Significance was assessed from biological replicates using two-sided Student's t-tests for unequal sample variance. P-values <0.05 were considered as significant.

Acknowledgements

We thank Sabine Rottmüller, Marion-Stefanie Roller, Dr. Martins Anton, Dr. Theo Thepen, Dr. Christoph Jan Wruck and Bernd Haas for technical assistance. This work was supported by the Max-Planck-Society, in part by the Behrens-Weise-Foundation, the European-Research-Council (ERC, grant 'sRNAs'), the NGFN+ Brain-Tumor-Network (No.01GS0887), the Deutsche Forschungsgemeinschaft (DFG, SFB 773-project A6 (to G.T.) and Me 2064/2-2 to G.M.), NCCR Neural plasticity and repair (P4), the START program of the University of Aachen (to C.B. and D.B.) and the Bavarian Ministry of Education and Science (BayGene to G.M.). L.W. received a fellowship of the Boehringer Ingelheim Fonds. D.B. is supported by a career award for young female scientists.

Conflict of interest

The authors declare that they have no conflict of interest

References

The Cancer Genome Atlas (TCGA) Research Network (2008) Comprehensive genomic characterization defines human glioblastoma genes and core pathways. *Nature* **455**(7216)**:** 1061-1068

Barbashina V, Salazar P, Holland EC, Rosenblum MK, Ladanyi M (2005) Allelic losses at 1p36 and 19q13 in gliomas: correlation with histologic classification, definition of a 150-kb minimal deleted region on 1p36, and evaluation of CAMTA1 as a candidate tumor suppressor gene. *Clin Cancer Res* **11**(3)**:** 1119-1128

Bartel DP (2009) MicroRNAs: target recognition and regulatory functions. *Cell* **136**(2)**:** 215-233

Beier D, Hau P, Proescholdt M, Lohmeier A, Wischhusen J, Oefner PJ, Aigner L, Brawanski A, Bogdahn U, Beier CP (2007) CD133(+) and CD133(-) glioblastoma-derived cancer stem cells show differential growth characteristics and molecular profiles. *Cancer Res* **67**(9)**:** 4010-4015

Beier D, Wischhusen J, Dietmaier W, Hau P, Proescholdt M, Brawanski A, Bogdahn U, Beier CP (2008) CD133 expression and cancer stem cells predict prognosis in high-grade oligodendroglial tumors. *Brain Pathol* **18**(3)**:** 370-377

Beitzinger M, Peters L, Zhu JY, Kremmer E, Meister G (2007) Identification of Human microRNA Targets From Isolated Argonaute Protein Complexes. *RNA Biol* **4**(2)

Bushati N, Cohen SM (2007) microRNA functions. *Annu Rev Cell Dev Biol* **23:** 175-205

Calin GA, Croce CM (2006) MicroRNA signatures in human cancers. *Nat Rev Cancer* **6**(11)**:** 857-866

Calin GA, Dumitru CD, Shimizu M, Bichi R, Zupo S, Noch E, Aldler H, Rattan S, Keating M, Rai K, Rassenti L, Kipps T, Negrini M, Bullrich F, Croce CM (2002) Frequent deletions and down-regulation of microRNA genes miR-15 and miR-16 at 13q14 in chronic lymphocytic leukemia. *Proc Natl Acad Sci U S A* **99**(24)**:** 15524-15529.

Carthew RW, Sontheimer EJ (2009) Origins and Mechanisms of miRNAs and siRNAs. *Cell* **136**(4)**:** 642-655

Chan JA, Krichevsky AM, Kosik KS (2005) MicroRNA-21 is an antiapoptotic factor in human glioblastoma cells. *Cancer Res* **65**(14)**:** 6029-6033

Costinean S, Zanesi N, Pekarsky Y, Tili E, Volinia S, Heerema N, Croce CM (2006) Pre-B cell proliferation and lymphoblastic leukemia/high-grade lymphoma in E(mu)-miR155 transgenic mice. *Proc Natl Acad Sci U S A* **103**(18)**:** 7024-7029

Croce CM (2009) Causes and consequences of microRNA dysregulation in cancer. *Nat Rev Genet* **10**(10)**:** 704-714

Delaloy C, Liu L, Lee JA, Su H, Shen F, Yang GY, Young WL, Ivey KN, Gao FB (2010) MicroRNA-9 coordinates proliferation and migration of human embryonic stem cell-derived neural progenitors. *Cell Stem Cell* **6**(4)**:** 323-335

Easow G, Teleman AA, Cohen SM (2007) Isolation of microRNA targets by miRNP immunopurification. *Rna* **13**(8)**:** 1198-1204

Esquela-Kerscher A, Slack FJ (2006) Oncomirs - microRNAs with a role in cancer. *Nat Rev Cancer* **6**(4)**:** 259-269

Finkler A, Ashery-Padan R, Fromm H (2007) CAMTAs: calmodulin-binding transcription activators from plants to human. *FEBS Lett* **581**(21)**:** 3893-3898

Garzon R, Calin GA, Croce CM (2009) MicroRNAs in Cancer. *Annu Rev Med* **60:** 167-179

Gilbertson RJ, Rich JN (2007) Making a tumour's bed: glioblastoma stem cells and the vascular niche. *Nat Rev Cancer* **7**(10)**:** 733-736

Han J, Gong P, Reddig K, Mitra M, Guo P, Li HS (2006) The fly CAMTA transcription factor potentiates deactivation of rhodopsin, a G protein-coupled light receptor. *Cell* **127**(4)**:** 847-858

He L, He X, Lim LP, de Stanchina E, Xuan Z, Liang Y, Xue W, Zender L, Magnus J, Ridzon D, Jackson AL, Linsley PS, Chen C, Lowe SW, Cleary MA, Hannon GJ (2007) A microRNA component of the p53 tumour suppressor network. *Nature* **447**(7148)**:** 1130-1134

He L, Thomson JM, Hemann MT, Hernando-Monge E, Mu D, Goodson S, Powers S, Cordon-Cardo C, Lowe SW, Hannon GJ, Hammond SM (2005) A microRNA polycistron as a potential human oncogene. *Nature* **435**(7043)**:** 828-833

Henrich KO, Bauer T, Schulte J, Ehemann V, Deubzer H, Gogolin S, Muth D, Fischer M, Benner A, Konig R, Schwab M, Westermann F (2011) CAMTA1, a 1p36 tumor suppressor candidate, inhibits growth and activates differentiation programs in neuroblastoma cells. *Cancer Res* **71**(8)**:** 3142-3151

Hock J, Weinmann L, Ender C, Rudel S, Kremmer E, Raabe M, Urlaub H, Meister G (2007) Proteomic and functional analysis of Argonaute-containing mRNA-protein complexes in human cells. *EMBO Rep* **8**(11)**:** 1052-1060

Huntzinger E, Izaurralde E (2011) Gene silencing by microRNAs: contributions of translational repression and mRNA decay. *Nat Rev Genet* **12**(2)**:** 99-110

Hurteau GJ, Spivack SD, Brock GJ (2006) Potential mRNA degradation targets of hsa-miR-200c, identified using informatics and qRT-PCR. *Cell Cycle* **5**(17)**:** 1951-1956

Huse JT, Brennan C, Hambardzumyan D, Wee B, Pena J, Rouhanifard SH, Sohn-Lee C, le Sage C, Agami R, Tuschl T, Holland EC (2009) The PTEN-regulating microRNA miR-26a is amplified in high-grade glioma and facilitates gliomagenesis in vivo. *Genes Dev* **23**(11)**:** 1327-1337

Huse JT, Phillips HS, Brennan CW (2011) Molecular subclassification of diffuse gliomas: Seeing order in the chaos. *Glia* **59**(8)**:** 1190-1199

Hutvagner G, Simard MJ (2008) Argonaute proteins: key players in RNA silencing. *Nat Rev Mol Cell Biol* **9**(1)**:** 22-32

Ichimura K, Vogazianou AP, Liu L, Pearson DM, Backlund LM, Plant K, Baird K, Langford CF, Gregory SG, Collins VP (2008) 1p36 is a preferential target of chromosome 1 deletions in astrocytic tumours and homozygously deleted in a subset of glioblastomas. *Oncogene* **27**(14)**:** 2097-2108

Ji Q, Hao X, Zhang M, Tang W, Yang M, Li L, Xiang D, Desano JT, Bommer GT, Fan D, Fearon ER, Lawrence TS, Xu L (2009) MicroRNA miR-34 inhibits human pancreatic cancer tumor-initiating cells. *PLoS ONE* **4**(8)**:** e6816

Johnson SM, Grosshans H, Shingara J, Byrom M, Jarvis R, Cheng A, Labourier E, Reinert KL, Brown D, Slack FJ (2005) RAS is regulated by the let-7 microRNA family. *Cell* **120**(5)**:** 635-647

Karginov FV, Conaco C, Xuan Z, Schmidt BH, Parker JS, Mandel G, Hannon GJ (2007) A biochemical approach to identifying microRNA targets. *Proc Natl Acad Sci U S A* **104**(49)**:** 19291-19296

Kim TM, Huang W, Park R, Park PJ, Johnson MD (2011) A Developmental Taxonomy of Glioblastoma Defined and Maintained by MicroRNAs. *Cancer Res* **71**(9)**:** 3387-3399

Kim VN, Han J, Siomi MC (2009) Biogenesis of small RNAs in animals. *Nat Rev Mol Cell Biol* **10**(2)**:** 126-139

Krol J, Loedige I, Filipowicz W (2010) The widespread regulation of microRNA biogenesis, function and decay. *Nat Rev Genet* **11**(9)**:** 597-610

Lagos-Quintana M, Rauhut R, Lendeckel W, Tuschl T (2001) Identification of novel genes coding for small expressed RNAs. *Science* **294**(5543)**:** 853-858

Leisegang M, Engels B, Meyerhuber P, Kieback E, Sommermeyer D, Xue SA, Reuss S, Stauss H, Uckert W (2008) Enhanced functionality of T cell receptor-redirected T cells is defined by the transgene cassette. *J Mol Med* **86**(5)**:** 573-583

Liu C, Kelnar K, Liu B, Chen X, Calhoun-Davis T, Li H, Patrawala L, Yan H, Jeter C, Honorio S, Wiggins JF, Bader AG, Fagin R, Brown D, Tang DG (2011) The microRNA miR-34a inhibits prostate cancer stem cells and metastasis by directly repressing CD44. *Nat Med* **17**(2)**:** 211-215

Livak KJ, Schmittgen TD (2001) Analysis of relative gene expression data using real-time quantitative PCR and the 2(-Delta Delta C(T)) Method. *Methods* **25**(4)**:** 402-408

Lobo NA, Shimono Y, Qian D, Clarke MF (2007) The biology of cancer stem cells. *Annu Rev Cell Dev Biol* **23:** 675-699

Lottaz C, Beier D, Meyer K, Kumar P, Hermann A, Schwarz J, Junker M, Oefner PJ, Bogdahn U, Wischhusen J, Spang R, Storch A, Beier CP (2010) Transcriptional profiles of CD133+ and CD133- glioblastoma-derived cancer stem cell lines suggest different cells of origin. *Cancer Res* **70**(5)**:** 2030-2040

Ma L, Young J, Prabhala H, Pan E, Mestdagh P, Muth D, Teruya-Feldstein J, Reinhardt F, Onder TT, Valastyan S, Westermann F, Speleman F, Vandesompele J, Weinberg RA (2010) miR-9, a MYC/MYCN-activated microRNA, regulates E-cadherin and cancer metastasis. *Nat Cell Biol* **12**(3)**:** 247-256

Madhavan S, Zenklusen JC, Kotliarov Y, Sahni H, Fine HA, Buetow K (2009) Rembrandt: helping personalized medicine become a reality through integrative translational research. *Mol Cancer Res* **7**(2)**:** 157-167

Malzkorn B, Wolter M, Liesenberg F, Grzendowski M, Stuhler K, Meyer HE, Reifenberger G (2010) Identification and functional characterization of microRNAs involved in the malignant progression of gliomas. *Brain Pathol* **20**(3)**:** 539-550

Mestdagh P, Fredlund E, Pattyn F, Schulte JH, Muth D, Vermeulen J, Kumps C, Schlierf S, De Preter K, Van Roy N, Noguera R, Laureys G, Schramm A, Eggert A, Westermann F, Speleman F, Vandesompele J (2010) MYCN/c-MYC-induced microRNAs repress coding gene networks associated with poor outcome in MYCN/c-MYC-activated tumors. *Oncogene* **29**(9)**:** 1394-1404

Nass D, Rosenwald S, Meiri E, Gilad S, Tabibian-Keissar H, Schlosberg A, Kuker H, Sion-Vardy N, Tobar A, Kharenko O, Sitbon E, Lithwick Yanai G, Elyakim E, Cholakh H, Gibori H, Spector Y, Bentwich Z, Barshack I, Rosenfeld N (2009) MiR-92b and miR-9/9* are specifically expressed in brain primary tumors and can be used to differentiate primary from metastatic brain tumors. *Brain Pathol* **19**(3)**:** 375-383

Nelson PT, Baldwin DA, Kloosterman WP, Kauppinen S, Plasterk RH, Mourelatos Z (2006) RAKE and LNA-ISH reveal microRNA expression and localization in archival human brain. *Rna* **12**(2)**:** 187-191

Packer AN, Xing Y, Harper SQ, Jones L, Davidson BL (2008) The bifunctional microRNA miR-9/miR-9* regulates REST and CoREST and is downregulated in Huntington's disease. *J Neurosci* **28**(53)**:** 14341-14346

Peters L, Meister G (2007) Argonaute proteins: mediators of RNA silencing. *Mol Cell* **26**(5)**:** 611-623

Phillips HS, Kharbanda S, Chen R, Forrest WF, Soriano RH, Wu TD, Misra A, Nigro JM, Colman H, Soroceanu L, Williams PM, Modrusan Z, Feuerstein BG, Aldape K (2006) Molecular subclasses of high-grade glioma predict prognosis, delineate a pattern of disease progression, and resemble stages in neurogenesis. *Cancer Cell* **9**(3)**:** 157-173

Reya T, Morrison SJ, Clarke MF, Weissman IL (2001) Stem cells, cancer, and cancer stem cells. *Nature* **414**(6859)**:** 105-111

Rudel S, Flatley A, Weinmann L, Kremmer E, Meister G (2008) A multifunctional human Argonaute2-specific monoclonal antibody. *Rna* **14**(6)**:** 1244-1253

Shimono Y, Zabala M, Cho RW, Lobo N, Dalerba P, Qian D, Diehn M, Liu H, Panula SP, Chiao E, Dirbas FM, Somlo G, Pera RA, Lao K, Clarke MF (2009) Downregulation of miRNA-200c links breast cancer stem cells with normal stem cells. *Cell* **138**(3)**:** 592-603

Song K, Backs J, McAnally J, Qi X, Gerard RD, Richardson JA, Hill JA, Bassel-Duby R, Olson EN (2006) The transcriptional coactivator CAMTA2 stimulates cardiac growth by opposing class II histone deacetylases. *Cell* **125**(3)**:** 453-466

Tabatabai G, Weller M (2011) Glioblastoma stem cells. *Cell Tissue Res* **343**(3)**:** 459-465

Tarasov V, Jung P, Verdoodt B, Lodygin D, Epanchintsev A, Menssen A, Meister G, Hermeking H (2007) Differential regulation of microRNAs by p53 revealed by massively parallel sequencing: miR-34a is a p53 target that induces apoptosis and G1-arrest. *Cell Cycle* **6**(13)**:** 1586-1593

Verhaak RG, Hoadley KA, Purdom E, Wang V, Qi Y, Wilkerson MD, Miller CR, Ding L, Golub T, Mesirov JP, Alexe G, Lawrence M, O'Kelly M, Tamayo P, Weir BA, Gabriel S, Winckler W, Gupta S, Jakkula L, Feiler HS, Hodgson JG, James CD, Sarkaria JN, Brennan C, Kahn A, Spellman PT, Wilson RK, Speed TP, Gray JW, Meyerson M, Getz G, Perou CM, Hayes DN (2010) Integrated genomic analysis identifies clinically relevant subtypes of glioblastoma characterized by abnormalities in PDGFRA, IDH1, EGFR, and NF1. *Cancer Cell* **17**(1)**:** 98-110

Vesely BA, Eichelbaum EJ, Alli AA, Sun Y, Gower WR, Jr., Vesely DL (2007) Four cardiac hormones eliminate 4-fold more human glioblastoma cells than the green mamba snake peptide. *Cancer Lett* **254**(1)**:** 94-101

Vesely BA, Song S, Sanchez-Ramos J, Fitz SR, Solivan SM, Gower WR, Jr., Vesely DL (2005) Four peptide hormones decrease the number of human breast adenocarcinoma cells. *Eur J Clin Invest* **35**(1)**:** 60-69

Visvader JE, Lindeman GJ (2008) Cancer stem cells in solid tumours: accumulating evidence and unresolved questions. *Nat Rev Cancer* **8**(10)**:** 755-768

Weinmann L, Hock J, Ivacevic T, Ohrt T, Mutze J, Schwille P, Kremmer E, Benes V, Urlaub H, Meister G (2009) Importin 8 is a gene silencing factor that targets argonaute proteins to distinct mRNAs. *Cell* **136**(3)**:** 496-507

Wong P, Iwasaki M, Somervaille TC, Ficara F, Carico C, Arnold C, Chen CZ, Cleary ML (2010) The miR-17-92 microRNA polycistron regulates MLL leukemia stem cell potential by modulating p21 expression. *Cancer Res* **70**(9)**:** 3833-3842

Wubbenhorst D, Dumler K, Wagner B, Wexel G, Imhoff A, Gansbacher B, Vogt S, Anton M (2010) Tetracycline-regulated bone morphogenetic protein 2 gene expression in lentivirally transduced primary rabbit chondrocytes for treatment of cartilage defects. *Arthritis Rheum* **62**(7)**:** 2037-2046

Yoo AS, Staahl BT, Chen L, Crabtree GR (2009) MicroRNA-mediated switching of chromatin-remodelling complexes in neural development. *Nature* **460**(7255)**:** 642-646

Yu F, Yao H, Zhu P, Zhang X, Pan Q, Gong C, Huang Y, Hu X, Su F, Lieberman J, Song E (2007) let-7 regulates self renewal and tumorigenicity of breast cancer cells. *Cell* **131**(6)**:** 1109-1123

Zhao C, Sun G, Li S, Shi Y (2009) A feedback regulatory loop involving microRNA-9 and nuclear receptor TLX in neural stem cell fate determination. *Nat Struct Mol Biol* **16**(4)**:** 365-371

Zhu L, Chen H, Zhou D, Li D, Bai R, Zheng S, Ge W (2011) MicroRNA-9 up-regulation is involved in colorectal cancer metastasis via promoting cell motility. *Med Oncol,* DOI: 10.1007/s12032-011-9975-z

Figure legends

Figure 1: miRNA expression profile of $CD133^+$ vs. $CD133^-$ glioblastoma cells. (A)/(B) Glioblastoma stem cells were sorted from primary glioblastoma cells (R11) and miRNA expression was analyzed by cloning and deep sequencing. (C) RNA composition of the libraries. (D) Comparison of the $CD133^+$ (positive value) and $CD133^-$ (negative value) miRNA expression profiles. The circle sizes indicate the abundance of the miRNA. (E) Validation of miR-17-5p, miR-9*, miR-106b and miR-9 in CD133+ glioblastoma cells (R11) by Northern blotting. Ile tRNA served as loading control. (F) Validation of the differential expression of miR-9 (upper panel), miR-9* (middle panel) and miR-34a (control, lower panel) in different glioblastoma cell lines.

Figure 2: miR-9/9* affect neurosphere formation and neuronal differentiation of glioblastoma stem cells. (A) miR-9*, miR-9, miR-17-5p and miR-106b were inhibited using 2'-O-methylated antisense oligonucleotides and neurosphere formation was analyzed in R11 cells. (B) A miR-9/9* mimic was transfected into primary glioblastoma cells (R11) and colony formation was analyzed. (C) Lower concentrations of inhibitors against miR-9/9* and miR-17 were co-transfected into R11 cells together with a control inhibitor or a miR-17 inhibitor and neurosphere formation was analyzed. (D) miR-9/9* were inhibited by antisense inhibitors in

primary glioblastoma cells (R11) and $CD133^+$ cells were analyzed by FACS. (E) miR-9/9* was inhibited as described above and the neuronal differentiation marker Tuj1 (upper panels), the glial differentiation marker GFAP (middle panels) were analyzed by Western blotting. β-actin (lower panels) was analyzed as loading control. In Figure 2A-E, significance was assessed by two-sided Student's t-test (* $p<0.05$, ** $p<0.01$, *** $p<0.001$, n.s. = not significant).

Figure 3: Identification of mir-9* target mRNAs. (A) Strategy to identify miR-9* target mRNAs. (B) List of most strongly Ago2-associated transcripts in primary glioblastoma cell line R11 in the presence of a miR-9* or miR-122 control inhibitor. miR-9* target mRNA candidates that were >10-fold depleted in the miR-9* inhibitor sample compared to the control are displayed in bold letters.

Figure 4: miR-9/9* regulate CAMTA1 expression. (A) Location of miR-9 (blue), miR-9* (red), miR-17-5p (yellow) and miR-106b (brown) on the 3' UTR of CAMTA1. (B) The CAMTA1 3' UTR or variants with mutated miR-9 (1) or miR-9* (2) binding sites were fused to luciferase and luciferase expression was investigated in the presence or absence of miR-9 (1) or miR-9* (2) inhibitors in T98G cells. Panel (3) shows inhibitory effects of miR-106b and miR-17-5p on the wild type CAMTA1 3' UTR. (C) mRNA levels of CAMTA1 were analyzed by qPCR upon miR-9 or miR-9* inhibition by antisense oligonucleotides in R11 cells. (D) CAMTA1 protein levels were analyzed upon miR-9 or miR-9* inhibition in R11 cells. Western blotting with a anti-β-actin antibody was used as loading control. (E) Primary glioblastoma cells (R11) were pre-treated with two different siRNAs against CAMTA1 for CAMTA1 depletion. Subsequently, neurosphere formation assays were performed as described in Figure 2A using miR-9 or miR-9* inhibitors.

Figure 5: CAMTA1 has tumor suppressor activity in vitro. (A) Domain organization of CAMTA1 and the CAMTA1ΔN, where the DNA-binding domain has been deleted. (B) Flag/HA-tagged CAMTA1 (FH-CAMTA1) as well as FH-CAMTA1ΔN was expressed in HEK 293T cells and protein expression was analyzed by Western blotting using an anti-CAMTA1 antibody. (C) FH-CAMTA1 was expressed in two different primary glioblastoma cells (R11, left panel and R28, right panel) and neurosphere formation was analyzed. (D) CAMTA1 and CAMTA1ΔN were expressed in R11 cells and neurosphere formation was analyzed. (E) CAMTA1 was expressed in primary glioblastoma cells (R11) and the $CD133^+$ cell population was analyzed by flow cytometry.

Figure 6: CAMTA1 regulates tumor growth in an *in vivo* xenograft model. R28 cells, stably transfected with luciferase, were transfected with pIRES or pIRES-CAMTA1. Cells were then intracranially injected into mice brains. Tumor growth was quantified by measurement of luciferase activity 15 days after implantation. (A) Dorsal views of two representative mice are depicted from pIRES and pIRES-CAMTA1 group. The color scales indicate the signal intensity at the surface of the animals recorded as total photons per second, square centimeter and steradian (p/s/cm2/sr). (B) Box-Plots of the quantified dorsal signals from both groups. Statistical significance was calculated with two-sided Student‘s ttest (* $p<0,05$).

Figure 7: CAMTA1 expression correlates with patient survival (A, B) CAMTA1 mRNA expression was analyzed in non-tumor brain tissue, WHO grade I-III astrocytoma and glioblastoma using the indicated affymetrix probes on a U-133A microarray. (C) Kaplan-Meier survival plot for glioblastoma patients with high, low and intermediate CAMTA1 mRNA expression, as determined by affymetrix probe 213268 on a U-133A microarray. Data were obtained from the Rembrandt and the TCGA databases (see Materials and Methods).

Figure 8. CAMTA1 regulates the peptide hormone NPPA and its receptor NPR-A. (A)/(B) CAMTA1 overexpression increases NPPA (A) and NPR-A mRNA levels (B). LNT-229 cells were transfected with indicated plasmids and NPPA or NPR-A mRNA levels were determined by qRT-PCR. Data were normalized to GAPDH mRNA levels as well as to the empty pIRES plasmid. (C) Inhibition of miR-9 and miR-9* increases NPPA and NPR-A mRNA levels. LNT-229 cells were transfected with indicated 2‘-O-methyl antisense oligonucleotides and NPPA or NPR-A mRNA levels were determined by qRT-PCR. Data were normalized to GAPDH mRNA levels and control inhibitor transfected samples. (D) NPPA expression correlates with glioma outcome. Kaplan-Meier survival plot for glioma patients (glioblastoma multiforme, oligodendroglioma, astrocytoma) with high, low and intermediate NPPA mRNA expression. Data were generated to Affymetrix probe 209957 on a U-133A microarray.

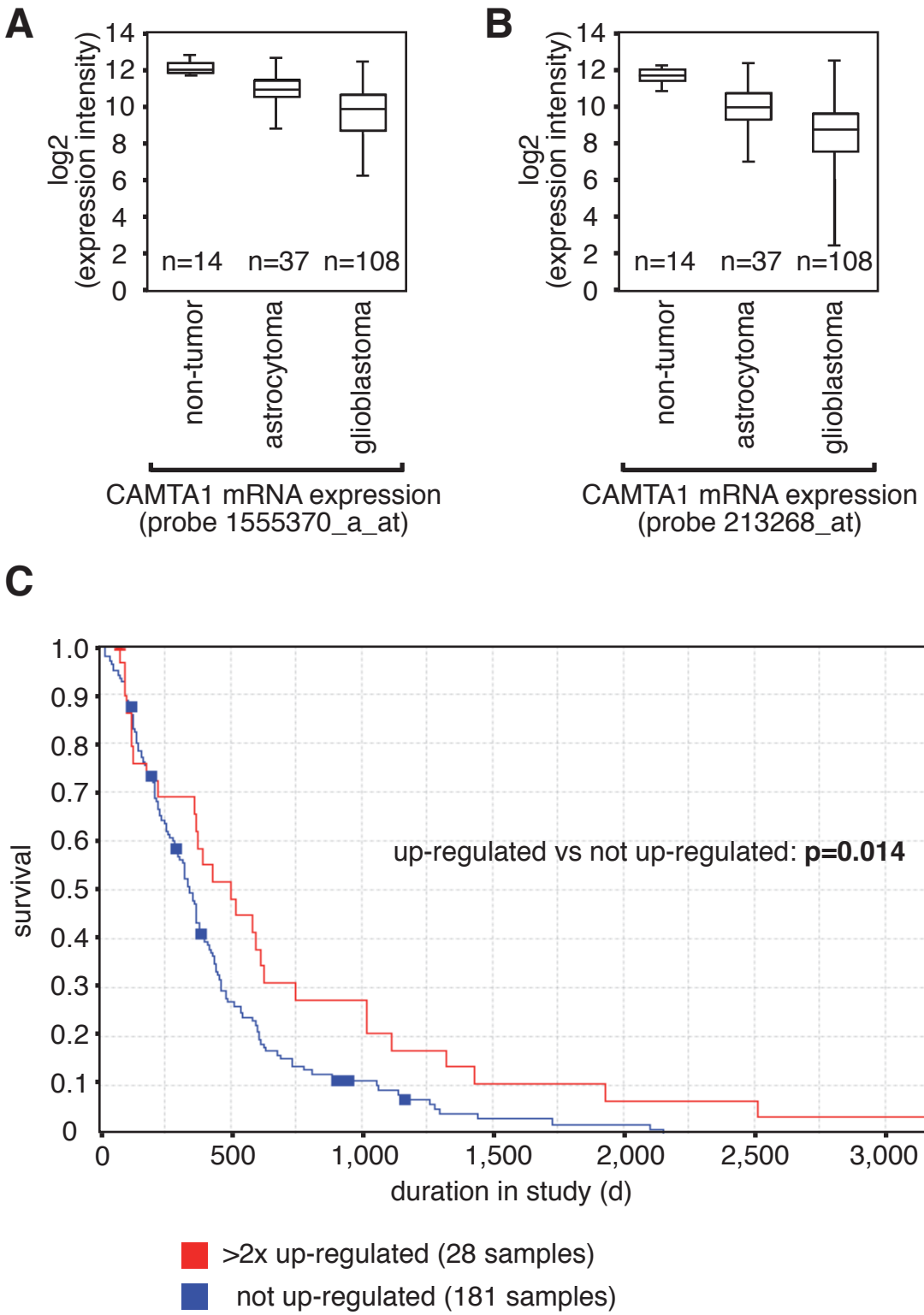
A
log2 (expression intensity)
14
12
10
8
6
4
2
0
n=14
n=37
n=108
non-tumor
astrocytoma
glioblastoma
CAMTA1 mRNA expression
(probe 1555370_a_at)
B
log2 (expression intensity)
n=14
n=37
n=108
non-tumor
astrocytoma
glioblastoma
CAMTA1 mRNA expression
(probe 213268_at)
C
survival
1.0
0.9
0.8
0.7
0.6
0.5
0.4
0.3
0.2
0.1
0
0
500
1,000
1,500
2,000
2,500
3,000
3,500
duration in study (d)
up-regulated vs not up-regulated: p=0.014
>2x up-regulated (28 samples)
not up-regulated (181 samples)

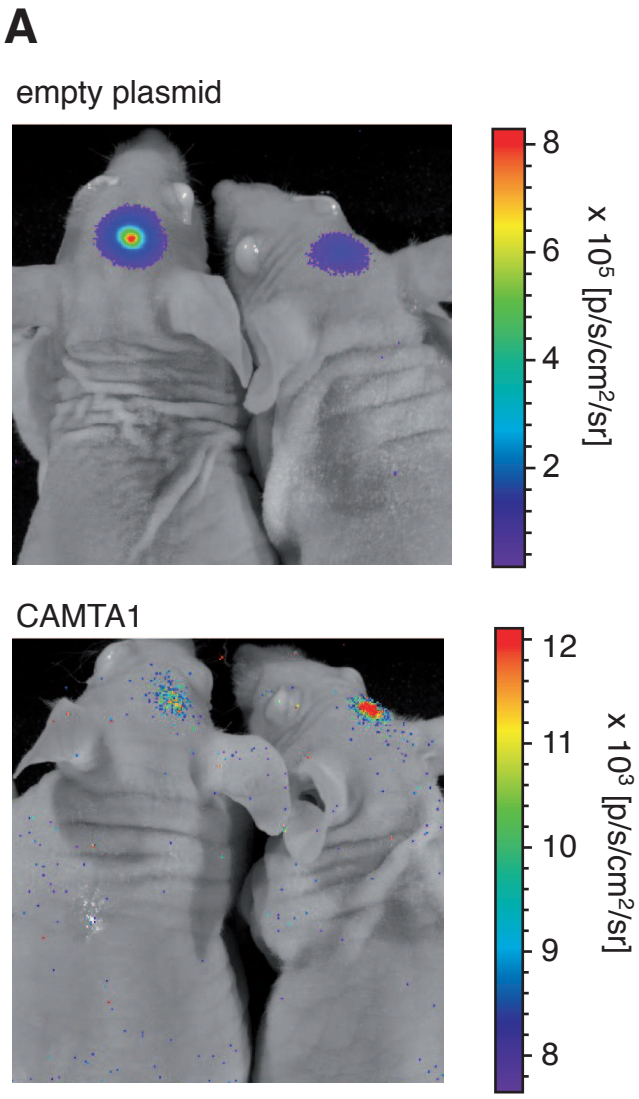
A
empty plasmid
8
6
4
2
x 10⁵ [p/s/cm²/sr]
CAMTA1
12
11
10
9
8
x 10³ [p/s/cm²/sr]
B
Bioluminescence x 10⁴ [p/s/cm²/sr]
7
6
5
4
3
2
1
0
n=12
n=13
*
pIRES plasmid:
empty
CAMTA1

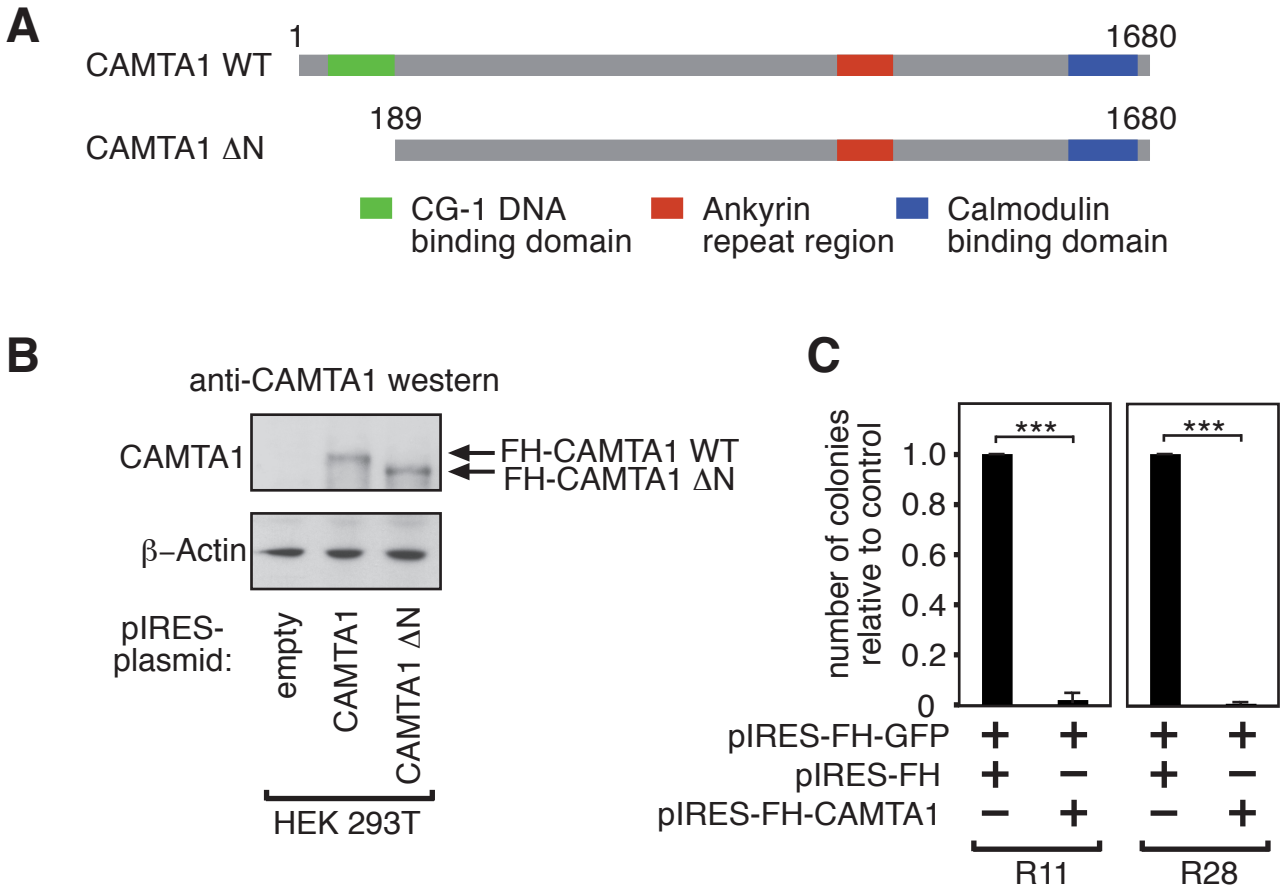
A
CAMTA1 WT
1
1680
CAMTA1 ΔN
189
1680
CG-1 DNA binding domain
Ankyrin repeat region
Calmodulin binding domain
B
anti-CAMTA1 western
CAMTA1
FH-CAMTA1 WT
FH-CAMTA1 ΔN
β–Actin
pIRES-plasmid:
empty
CAMTA1
CAMTA1 ΔN
HEK 293T
C
number of colonies relative to control
1.0
0.8
0.6
0.4
0.2
0
***
***
pIRES-FH-GFP
pIRES-FH
pIRES-FH-CAMTA1
R11
R28
D
number of colonies relative to control
1.4
1.2
1.0
0.8
0.6
0.4
0.2
0
*
***
pIRES-plasmid:
empty plasmid
CAMTA1 WT
CAMTA1 ΔN
E
relative number of CD133+ cells
1.0
0.8
0.6
0.4
0.2
0
*
pIRES-plasmid:
empty
CAMTA1

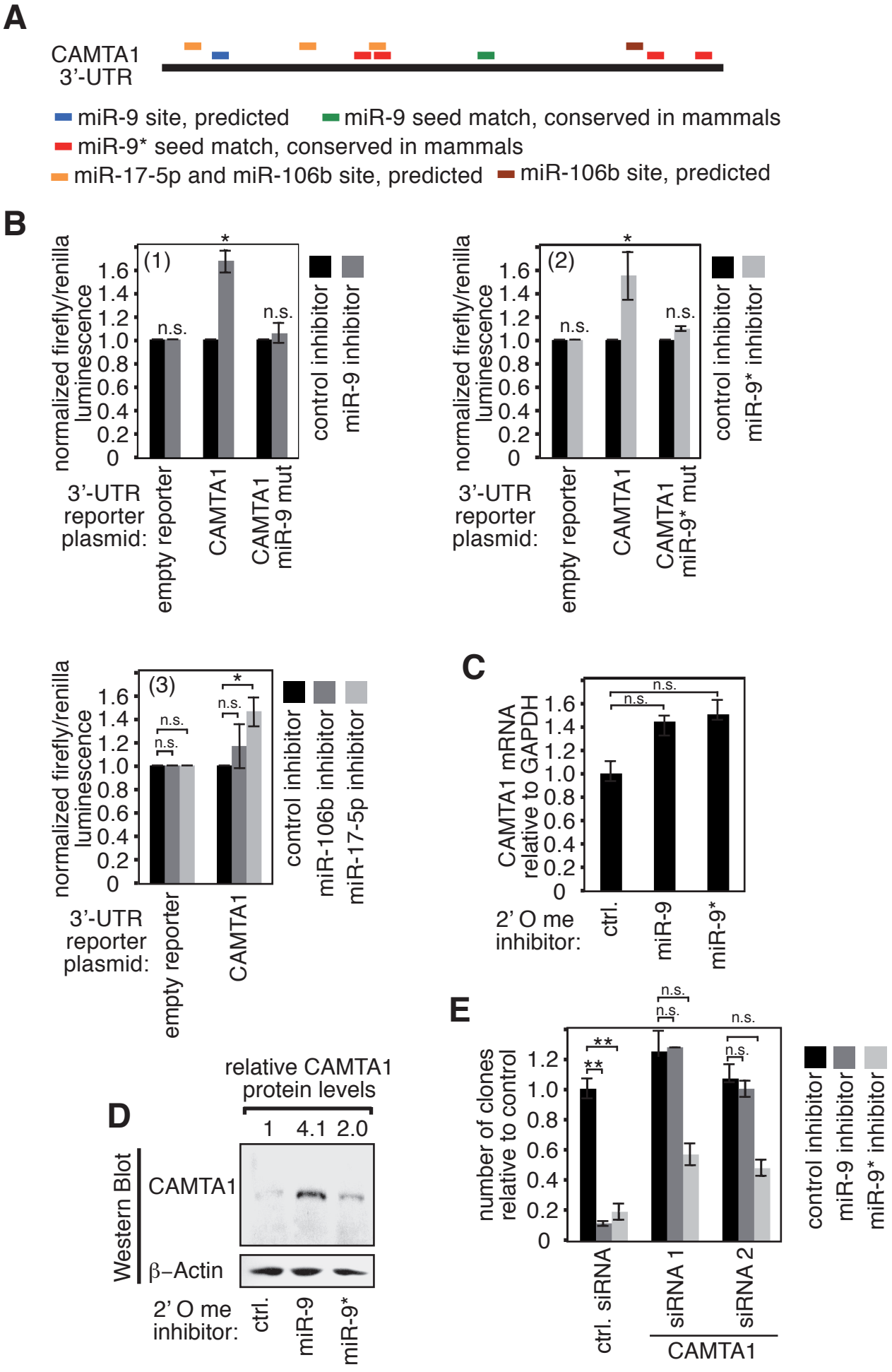
A
CAMTA1
3'-UTR
miR-9 site, predicted
miR-9 seed match, conserved in mammals
miR-9* seed match, conserved in mammals
miR-17-5p and miR-106b site, predicted
miR-106b site, predicted
B
(1)
normalized firefly/renilla luminescence
3'-UTR reporter plasmid:
empty reporter
CAMTA1
CAMTA1 miR-9 mut
control inhibitor
miR-9 inhibitor
n.s.
*
(2)
CAMTA1 miR-9* mut
miR-9* inhibitor
(3)
miR-106b inhibitor
miR-17-5p inhibitor
C
CAMTA1 mRNA relative to GAPDH
2' O me inhibitor:
ctrl.
miR-9
miR-9*
D
relative CAMTA1 protein levels
1
4.1
2.0
Western Blot
CAMTA1
β–Actin
E
number of clones relative to control
**
ctrl. siRNA
siRNA 1
siRNA 2
CAMTA1

A

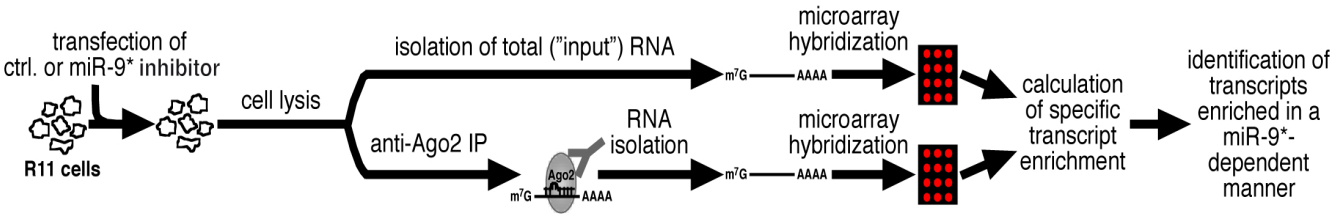

B

Agilent probe ID	fold mRNA enrichment, miR-122 inhibitor sample	fold mRNA enrichment, miR-9* inhibitor sample	NCBI accession	gene name	fold change
A_23_P334777	**41.41**	**3.70**	**NM_170725**	**PGBD2**	37.71
A_24_P264832	**27.81**	**0.85**	**NM_005382**	**NEFM**	26.96
A_32_P46154	33.19	8.28	NM_021269	ZNF708	24.91
A_23_P91943	28.95	5.16	NM_000882	IL12A	23.79
A_23_P96008	**23.33**	**0.55**	**NM_006785**	**MALT1**	22.78
A_24_P220921	**19.98**	**0.40**	**NM_015215**	**CAMTA1**	19.58
A_23_P83007	22.57	5.50	NM_203403	C9orf150	17.07
A_23_P139786	**16.30**	**0.16**	**NM_003733**	**OASL**	16.14
A_23_P205818	**16.49**	**0.36**	**NM_014659**	**HISPPD2A**	16.13
A_23_P152330	17.32	1.79	NM_003586	DOC2A	15.53
A_24_P626470	**15.95**	**0.72**	**AA918648**		15.23
A_24_P177553	15.33	2.21	NR_003125	LOC85391	13.12
A_32_P164246	16.51	5.11	NM_033260	FOXQ1	11.40
A_24_P42446	16.72	7.13	NM_001015508	PURG	9.59
A_23_P2307	23.63	15.54	NM_144593	RHEBL1	8.09
A_23_P501080	15.73	8.07	NM_007139	ZNF92	7.66
A_24_P37409	16.49	9.60	NM_004418	DUSP2	6.90
A_23_P95930	19.96	13.91	NM_003483	HMGA2	6.05
A_23_P62901	15.63	10.99	NM_006763	BTG2	4.64
A_23_P383132	18.34	15.58	NM_015094	HIC2	2.76

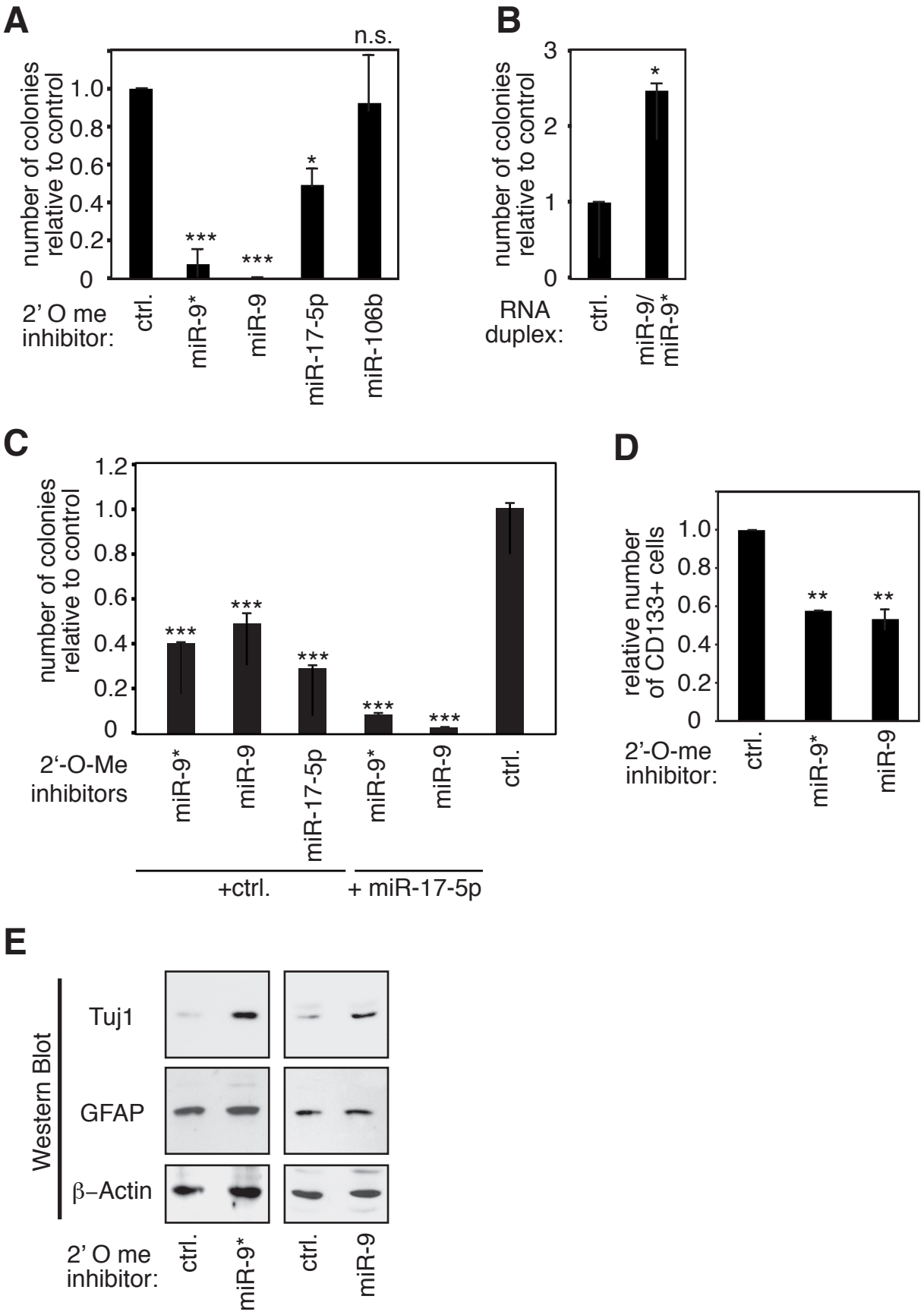
A
number of colonies relative to control
1.0
0.8
0.6
0.4
0.2
0
***
***
*
n.s.
2' O me inhibitor:
ctrl.
miR-9*
miR-9
miR-17-5p
miR-106b
B
number of colonies relative to control
3
2
1
0
*
RNA duplex:
ctrl.
miR-9/ miR-9*
C
number of colonies relative to control
1.2
1.0
0.8
0.6
0.4
0.2
0
***
***
***
***
***
2'-O-Me inhibitors
miR-9*
miR-9
miR-17-5p
miR-9*
miR-9
ctrl.
+ctrl.
+ miR-17-5p
D
relative number of CD133+ cells
1.0
0.8
0.6
0.4
0.2
0
**
**
2'-O-me inhibitor:
ctrl.
miR-9*
miR-9
E
Western Blot
Tuj1
GFAP
β–Actin
2' O me inhibitor:
ctrl.
miR-9*
ctrl.
miR-9

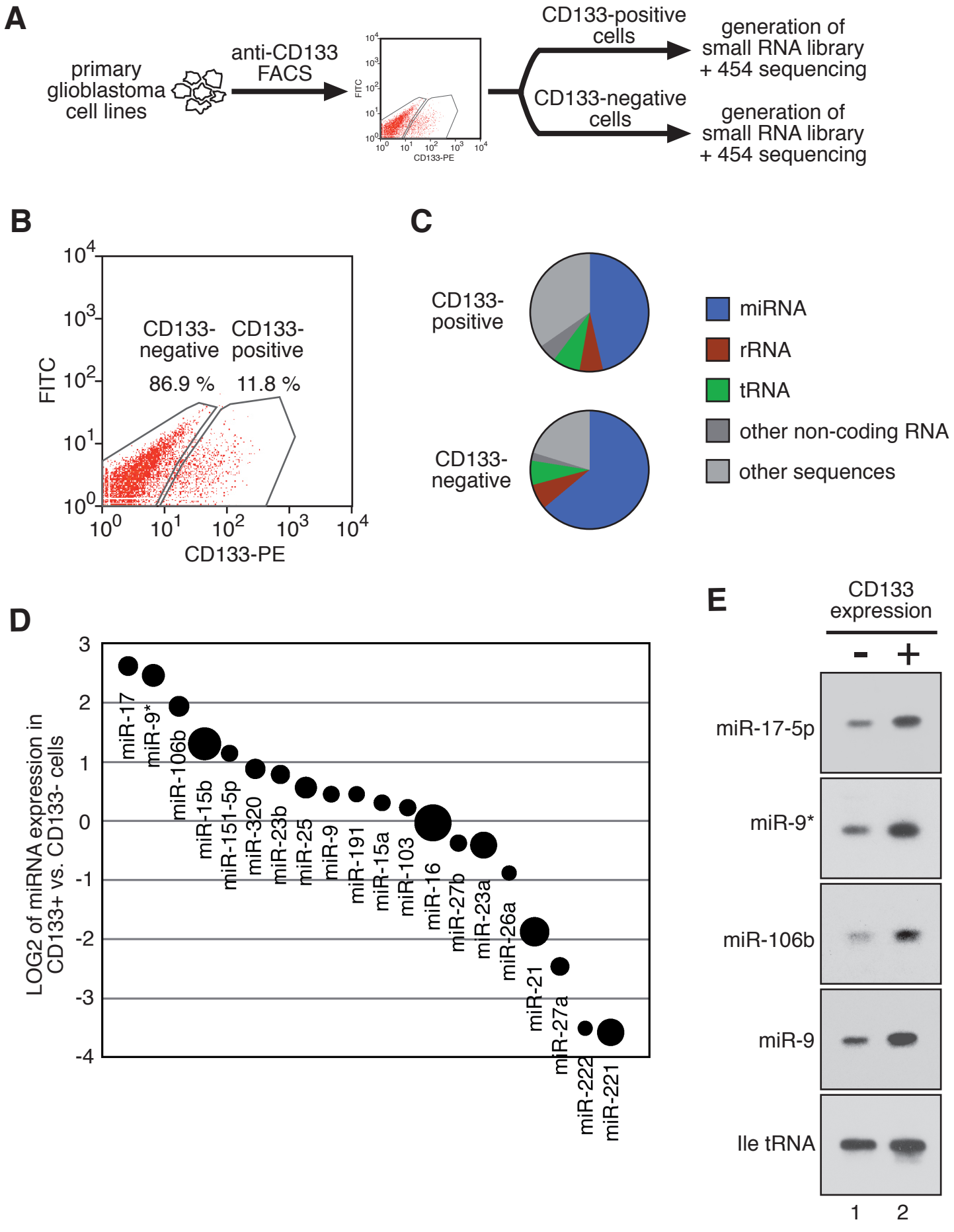
A
primary glioblastoma cell lines
anti-CD133 FACS
FITC
CD133-PE
CD133-positive cells
CD133-negative cells
generation of small RNA library + 454 sequencing
generation of small RNA library + 454 sequencing
B
CD133- negative
CD133- positive
86.9 %
11.8 %
FITC
CD133-PE
C
CD133- positive
CD133- negative
miRNA
rRNA
tRNA
other non-coding RNA
other sequences
D
LOG2 of miRNA expression in CD133+ vs. CD133- cells
miR-17
miR-9*
miR-106b
miR-15b
miR-151-5p
miR-320
miR-23b
miR-25
miR-9
miR-191
miR-15a
miR-103
miR-16
miR-27b
miR-23a
miR-26a
miR-21
miR-27a
miR-222
miR-221
E
CD133 expression
-
+
miR-17-5p
miR-9*
miR-106b
miR-9
Ile tRNA
1
2

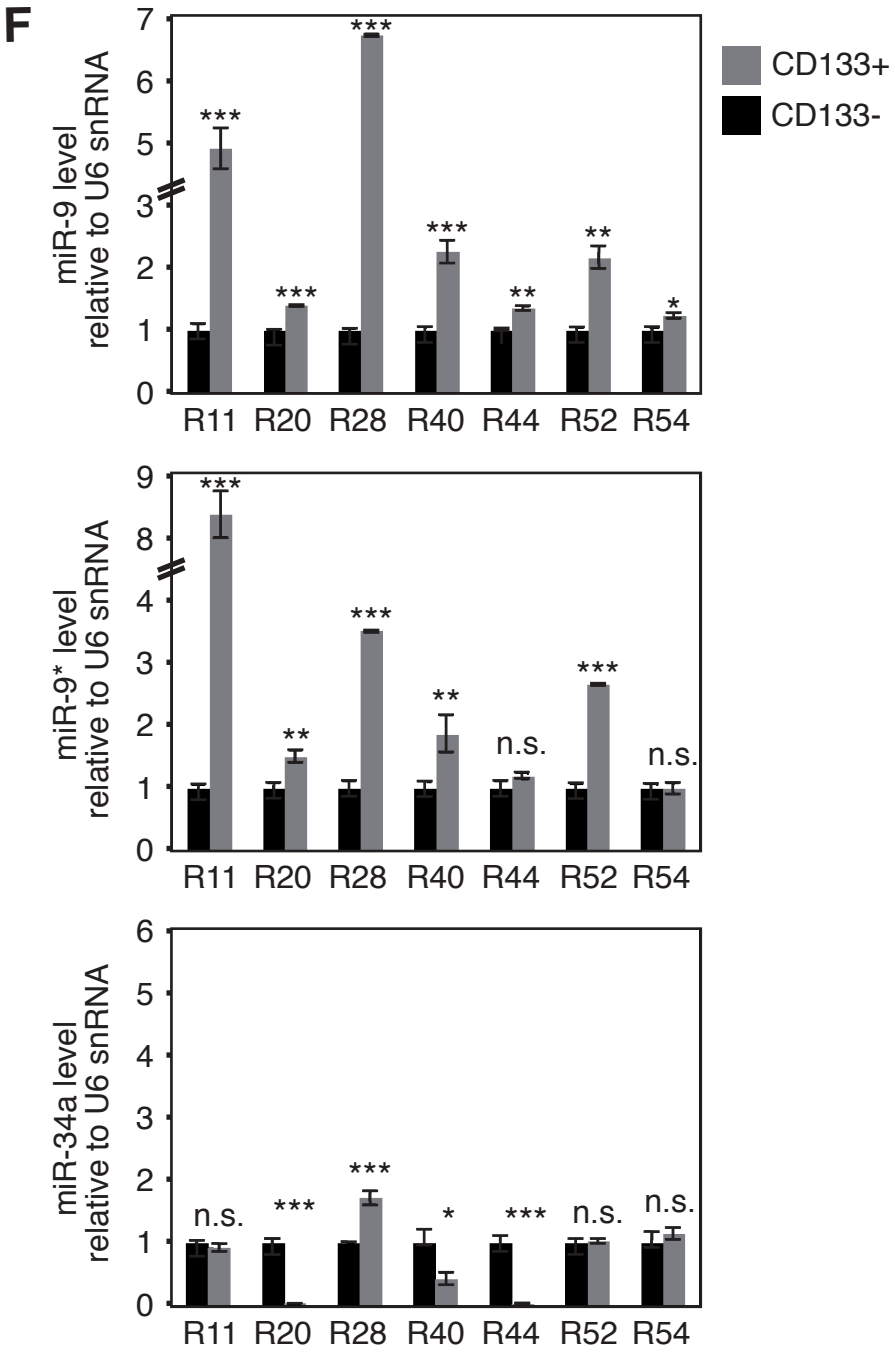
F
CD133+
CD133-
miR-9 level relative to U6 snRNA
miR-9* level relative to U6 snRNA
miR-34a level relative to U6 snRNA
R11 R20 R28 R40 R44 R52 R54
***
**
*
n.s.

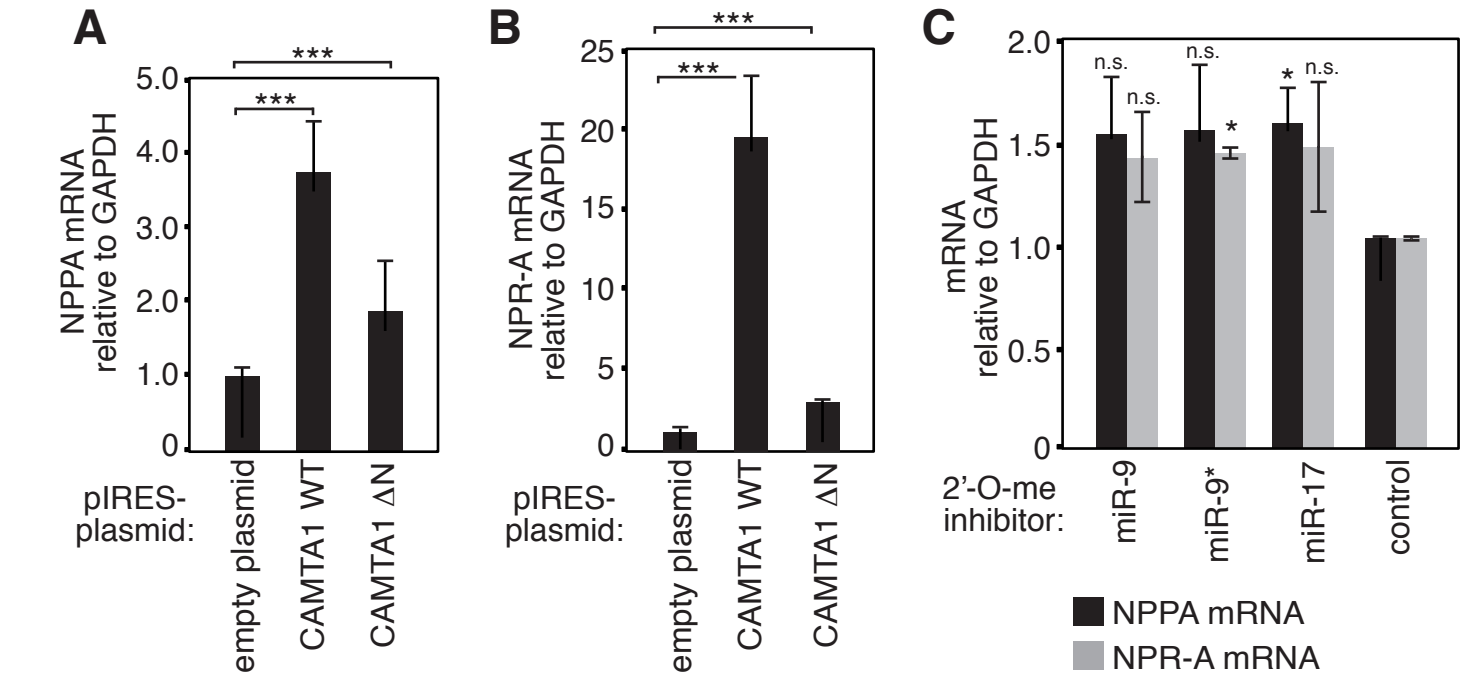
A
NPPA mRNA relative to GAPDH
5.0
4.0
3.0
2.0
1.0
0
***
***
pIRES-plasmid:
empty plasmid
CAMTA1 WT
CAMTA1 ΔN
B
NPR-A mRNA relative to GAPDH
25
20
15
10
5
0
***
***
pIRES-plasmid:
empty plasmid
CAMTA1 WT
CAMTA1 ΔN
C
mRNA relative to GAPDH
2.0
1.5
1.0
0.5
0
n.s.
n.s.
n.s.
*
*
n.s.
2'-O-me inhibitor:
miR-9
miR-9*
miR-17
control
NPPA mRNA
NPR-A mRNA

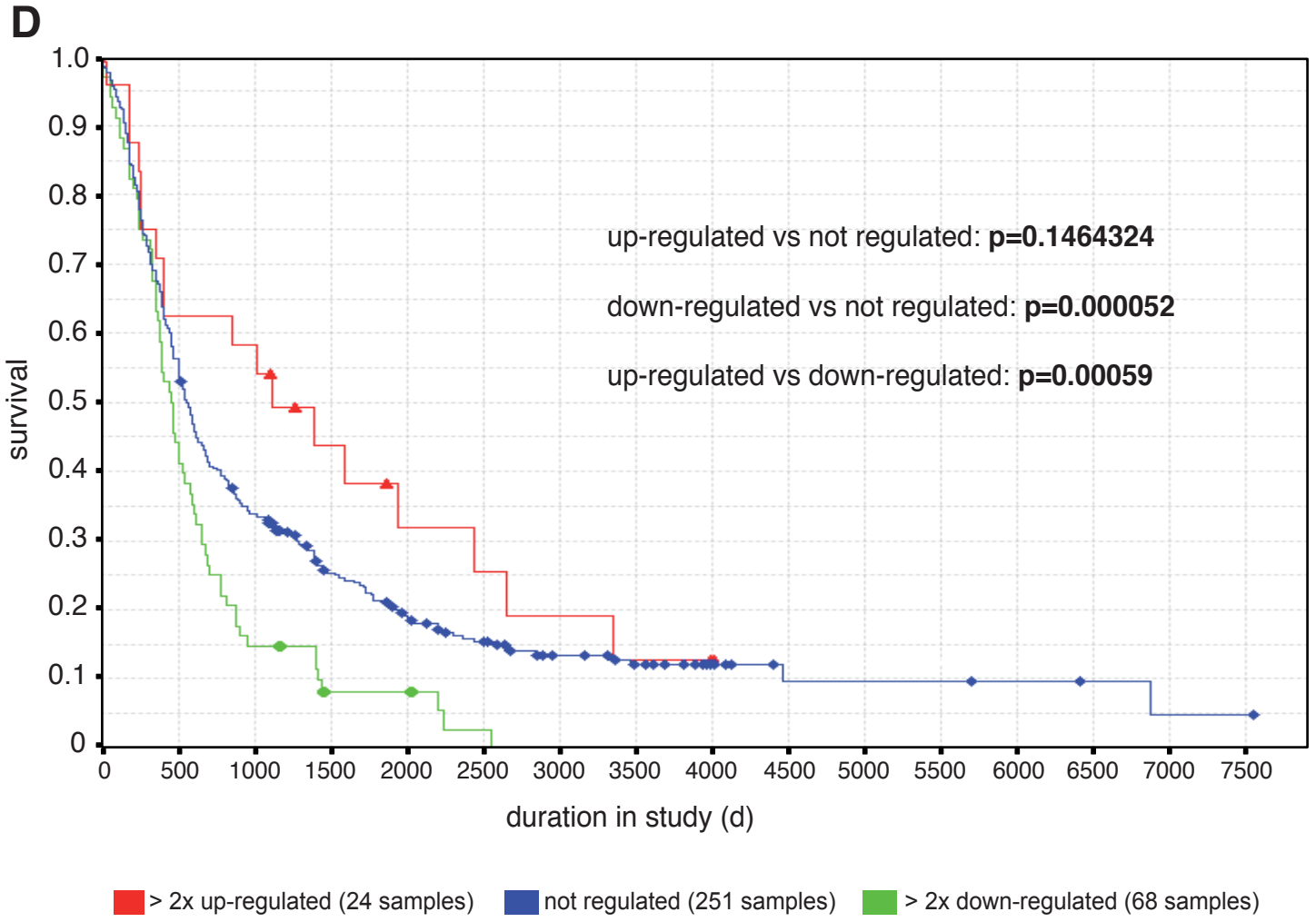
D
survival
1.0
0.9
0.8
0.7
0.6
0.5
0.4
0.3
0.2
0.1
0
0
500
1000
1500
2000
2500
3000
3500
4000
4500
5000
5500
6000
6500
7000
7500
duration in study (d)
up-regulated vs not regulated: p=0.1464324
down-regulated vs not regulated: p=0.000052
up-regulated vs down-regulated: p=0.00059
> 2x up-regulated (24 samples)
not regulated (251 samples)
> 2x down-regulated (68 samples)

CAMTA1 is a novel tumor suppressor regulated by miR-9/9* in glioblastoma stem cells

Daniel Schraivogel[1]#, Lasse Weinmann[2,3]#, Dagmar Beier[4,5], Ghazaleh Tabatabai[6], Alexander Eichner[7], Jia Yun Zhu[2], Michael Sixt[7], Martina Anton[8], Michael Weller[6], Christoph P. Beier[4,5] & Gunter Meister[1,2]*

Supplementary material

Supplementary Figure legends

Supplemental Figure 1: miR-9 and miR-9* can be independently depleted by using 2'-O-methyl antisense oligonucleotides. A) R11 cells were transfected twice with antagomirs. RNA was isolated and miRNA levels were analyzed by qPCR relative to U6 snRNA expression and to control inhibitor-transfected samples. B) R11 cells were treated as in A. RNA was isolated and analyzed for hsa-miR-9 and hsa-miR-9* levels by Northern Blotting, using Ile tRNA as loading control.

Supplemental Figure 2: CAMTA1 knockdown in R11 cells. R11 cells were transfected with two different CAMTA1 siRNAs. A) CAMTA1 mRNA levels were quantified by qRT-PCR and normalized to GAPDH. B) Levels of endogenous CAMTA1 protein and β-Actin were analyzed by Western Blotting. C) The CAMTA1 signals obtained by Western Blotting were quantified relative to β-Actin signals.

Supplemental Figure 3: CAMTA1 mRNA expression in CD133+ and CD133- cells. (A) CD133+ and CD133- cells of the indicated cell lines (R11, R28, R40, R44, R54) were separated by FACS sorting, mRNA was extracted and CAMTA1 mRNA levels were determined by qPCR. (B) CD133+ and CD133- cells derived from the R28 cell line were

analyzed by western blotting with antibodies against CAMTA1 (upper panel) or ß-actin (lower panel).

Supplemental table 1: Composition of the individual deep sequencing libraries

	reads	reads
RNA class	**CD133-negative cells**	**CD133-positive cells**
total reads	76339	65536
miRNA	48834	30452
rRNA	5253	4060
tRNA	5144	4924
other noncoding RNAs	1699	3303
other sequences	15409	22797

Supplemental table 2: miRNA composition of the individual deep sequencing libraries

miRNA	reads (CD133-)	reads (CD133+)	reads (both libraries)
hsa-miR-16	4829	2954	7783
hsa-miR-15b	2443	3774	6217
hsa-miR-21	4129	704	4833
hsa-miR-221	3973	208	4181
hsa-miR-23a	2763	1299	4062
hsa-miR-9*	653	2250	2903
hsa-miR-25	1402	1294	2696
hsa-miR-106b	704	1688	2392
hsa-miR-320	1035	1191	2226
hsa-miR-17	441	1691	2132
hsa-miR-23b	1005	1084	2089
hsa-miR-27a	1853	210	2063
hsa-miR-151-5p	688	948	1636
hsa-miR-27b	1099	530	1629
hsa-miR-103	1041	728	1769
hsa-miR-9	841	719	1560
hsa-miR-15a	871	673	1544
hsa-miR-191	750	641	1391
hsa-miR-26a	963	327	1290
hsa-miR-222	1166	64	1230
hsa-miR-92a	479	519	998
hsa-let-7a	550	428	978
hsa-miR-93	550	402	952
hsa-miR-424	528	392	920
hsa-miR-26b	478	383	861
hsa-miR-20a	422	392	814
hsa-miR-31	733	13	746
hsa-miR-24	639	65	704
hsa-miR-374b	277	351	628
hsa-miR-30b	475	82	557
hsa-miR-125b	370	149	519
hsa-miR-195	353	154	507
hsa-miR-29a	415	79	494
hsa-let-7b	387	93	480
hsa-miR-30c	408	61	469
hsa-miR-128a	120	342	462
hsa-miR-204	422	11	433
hsa-miR-34a	427	5	432
hsa-miR-151-3p	287	139	426
hsa-miR-31*	398	4	402
hsa-miR-361-5p	183	191	374
hsa-miR-92b	201	130	331
hsa-let-7g	206	79	285
hsa-miR-497	244	41	285
hsa-let-7f	223	44	267
hsa-miR-140-3p	146	96	242
hsa-miR-199a-3p	127	102	229
hsa-miR-423-3p	178	49	227
hsa-miR-125a-5p	177	49	226
hsa-miR-152	185	41	226

hsa-miR-22	199	22	221
hsa-miR-196a	42	122	164
hsa-miR-30d	153	10	163
hsa-let-7c	127	33	160
hsa-let-7d*	51	103	154
hsa-miR-378	129	22	151
hsa-miR-345	100	50	150
hsa-miR-28-5p	116	30	146
hsa-miR-153	126	18	144
hsa-miR-21*	119	22	141
hsa-miR-30a	133	8	141
hsa-miR-28-3p	90	47	137
hsa-miR-20b	54	79	133
hsa-miR-130b	82	48	130
hsa-miR-99b	79	49	128
hsa-miR-484	111	16	127
hsa-miR-99a	90	27	117
hsa-miR-149	113	2	115
hsa-miR-185	71	44	115
hsa-miR-374a	102	13	115
hsa-miR-425	63	52	115
hsa-miR-148a	108	4	112
hsa-miR-22*	76	35	111
hsa-miR-29c	86	23	109
hsa-miR-130a	66	38	104
hsa-miR-17*	46	58	104
hsa-miR-652	55	49	104
hsa-miR-181b	83	20	103
hsa-miR-30a*	66	35	101
hsa-miR-30e	79	19	98
hsa-miR-106a	31	61	92
hsa-miR-190	58	34	92
hsa-miR-210	16	76	92
hsa-miR-218	81	11	92
hsa-miR-455-3p	72	20	92
hsa-miR-16-2*	78	13	91
hsa-miR-182	44	46	90
hsa-miR-450a	81	9	90
hsa-miR-106b*	37	43	80
hsa-miR-100	63	13	76
hsa-miR-30e*	29	42	71
hsa-let-7b*	60	8	68
hsa-miR-181a	50	17	67
hsa-miR-532-3p	27	36	63
hsa-miR-101	37	25	62
hsa-let-7e	34	26	60
hsa-miR-187	56	4	60
hsa-miR-590-3p	44	16	60
hsa-miR-532-5p	21	38	59
hsa-miR-107	135	90	225
hsa-miR-671-5p	55	3	58
hsa-miR-744	35	23	58
hsa-miR-324-3p	34	22	56
hsa-miR-183	19	35	54

hsa-miR-221*	45	8	53
hsa-miR-155	48	4	52
hsa-miR-454	39	11	50
hsa-let-7a*	45	4	49
hsa-let-7d	20	29	49
hsa-miR-199a-5p	48	0	48
hsa-miR-103-2*	21	26	47
hsa-miR-138	22	25	47
hsa-miR-424*	25	21	46
hsa-miR-582-5p	44	2	46
hsa-let-7i	40	5	45
hsa-miR-193b	39	6	45
hsa-mir-1271	20	23	43
hsa-miR-488	8	34	42
hsa-miR-301a	30	10	40
hsa-miR-615-3p	9	29	38
hsa-miR-887	28	10	38
hsa-miR-19b	33	3	36
hsa-miR-503	19	17	36
hsa-miR-378*	24	11	35
hsa-miR-423-5p	24	9	33
hsa-miR-138-1*	6	26	32
hsa-miR-1307	21	11	32
hsa-miR-140-5p	23	9	32
hsa-miR-574-3p	26	4	30
hsa-let-7f-1*	22	7	29
hsa-miR-365	27	1	28
hsa-miR-340*	5	21	26
hsa-let-7f-2*	12	13	25
hsa-miR-10b	14	11	25
hsa-miR-132	12	13	25
hsa-miR-148b	22	2	24
hsa-miR-186	22	2	24
hsa-miR-342-3p	23	1	24
hsa-miR-145	22	0	22
hsa-miR-421	16	6	22
hsa-miR-598	8	14	22
hsa-miR-7-1*	5	17	22
hsa-miR-505	20	1	21
hsa-miR-197	15	4	19
hsa-miR-200c	13	6	19
hsa-miR-339-3p	19	0	19
hsa-miR-34b*	17	1	18
hsa-miR-224	12	5	17
hsa-miR-29b	13	4	17
hsa-miR-483-5p	0	17	17
hsa-miR-500*	9	8	17
hsa-miR-590-5p	16	1	17
hsa-miR-339-5p	16	0	16
hsa-miR-340	3	12	15
hsa-miR-361-3p	12	3	15
hsa-miR-574-5p	8	7	15
hsa-miR-886-5p	10	5	15
hsa-miR-98	9	6	15

hsa-miR-766	9	5	14
hsa-miR-99a*	12	2	14
hsa-miR-328	13	0	13
hsa-miR-33a*	11	2	13
hsa-miR-362-3p	13	0	13
hsa-miR-500	3	10	13
hsa-miR-584	8	5	13
hsa-miR-769-5p	10	3	13
hsa-miR-93*	12	1	13
hsa-let-7e*	4	8	12
hsa-miR-125b-2*	10	2	12
hsa-miR-181a-2*	3	9	12
hsa-miR-96	10	2	12
hsa-miR-146b-5p	9	2	11
hsa-miR-324-5p	7	4	11
hsa-miR-363	7	4	11
hsa-miR-95	0	11	11
hsa-let-7i*	10	0	10
hsa-miR-10a	10	0	10
hsa-miR-124	1	9	10
hsa-miR-181d	5	5	10
hsa-miR-34c-3p	9	1	10
hsa-miR-34c-5p	10	0	10
hsa-miR-551b	2	8	10
hsa-miR-190b	0	9	9
hsa-miR-205	9	0	9
hsa-miR-335	6	3	9
hsa-miR-501-3p	6	3	9
hsa-miR-768-3p	8	1	9
hsa-miR-15b*	8	0	8
hsa-miR-301b	8	0	8
hsa-miR-362-5p	8	0	8
hsa-miR-550	6	2	8
hsa-miR-671-3p	7	1	8
hsa-miR-675	0	8	8
hsa-miR-125a-3p	6	1	7
hsa-miR-130b*	3	4	7
hsa-miR-194	6	1	7
hsa-miR-214	7	0	7
hsa-miR-296-3p	3	4	7
hsa-miR-32	7	0	7
hsa-miR-199b-5p	2	4	6
hsa-miR-483-3p	0	6	6
hsa-miR-486-5p	4	2	6
hsa-miR-550*	6	0	6
hsa-miR-7	4	2	6
hsa-miR-132*	4	1	5
hsa-miR-181c*	0	5	5
hsa-miR-18a	2	3	5
hsa-miR-18b	2	3	5
hsa-miR-193a-3p	5	0	5
hsa-miR-200b	4	1	5
hsa-miR-23b*	3	2	5
hsa-miR-29b-1*	5	0	5

hsa-miR-335*	5	0	5
hsa-miR-33b*	2	3	5
hsa-miR-374b*	3	2	5
hsa-miR-455-5p	5	0	5
hsa-miR-502-5p	0	5	5
hsa-miR-624*	4	1	5
hsa-miR-708	3	2	5
hsa-miR-769-3p	3	2	5
hsa-miR-886-3p	5	0	5
hsa-miR-92b*	3	2	5
hsa-miR-935	1	4	5
hsa-let-7g*	3	1	4
hsa-miR-126	2	2	4
hsa-miR-135b	4	0	4
hsa-miR-212	2	2	4
hsa-miR-25*	3	1	4
hsa-miR-27b*	2	2	4
hsa-miR-29a*	4	0	4
hsa-miR-331-3p	3	1	4
hsa-miR-34b	3	1	4
hsa-miR-501-5p	4	0	4
hsa-miR-513-5p	4	0	4
hsa-miR-628-3p	1	3	4
hsa-miR-874	3	1	4
hsa-miR-942	3	1	4
hsa-miR-125b-1*	2	1	3
hsa-miR-137	3	0	3
hsa-miR-139-5p	0	3	3
hsa-miR-146a	2	1	3
hsa-miR-18a*	2	1	3
hsa-miR-32*	1	2	3
hsa-miR-330-3p	0	3	3
hsa-miR-338-3p	0	3	3
hsa-miR-34a*	2	1	3
hsa-miR-425*	2	1	3
hsa-miR-542-3p	3	0	3
hsa-miR-628-5p	2	1	3
hsa-miR-767-3p	0	3	3
hsa-miR-877	1	2	3
hsa-miR-885-5p	3	0	3
hsa-miR-99b*	1	2	3
hsa-mR-199a-3p	3	0	3
hsa-miR-126*	0	2	2
hsa-miR-135a	0	2	2
hsa-miR-146b-3p	2	0	2
hsa-miR-149*	1	1	2
hsa-miR-15a*	1	1	2
hsa-miR-181a*	1	1	2
hsa-miR-193b*	2	0	2
hsa-miR-20b*	1	1	2
hsa-miR-219-5p	2	0	2
hsa-miR-30d*	1	1	2
hsa-miR-326	1	1	2
hsa-miR-331-5p	1	1	2

hsa-miR-488*	0	2	2
hsa-miR-551b*	2	0	2
hsa-miR-582-3p	1	1	2
hsa-miR-643	0	2	2
hsa-miR-660	2	0	2
hsa-miR-760	2	0	2
hsa-miR-885-3p	0	2	2
hsa-miR-888	0	2	2
hsa-miR-940	1	1	2
hsa-miR-941	2	0	2
hsa-miR-100*	1	0	1
hsa-miR-105	0	1	1
hsa-miR-10a*	1	0	1
hsa-miR-129*	0	1	1
hsa-miR-129-5p	1	0	1
hsa-miR-135a*	0	1	1
hsa-miR-135b*	1	0	1
hsa-miR-138-2*	0	1	1
hsa-miR-141	1	0	1
hsa-miR-143	1	0	1
hsa-miR-143*	1	0	1
hsa-miR-181c	0	1	1
hsa-miR-183*	0	1	1
hsa-miR-184	0	1	1
hsa-miR-192	0	1	1
hsa-miR-193a-5p	1	0	1
hsa-miR-195*	1	0	1
hsa-miR-20a*	1	0	1
hsa-miR-219-1-3p	0	1	1
hsa-miR-24-1*	0	1	1
hsa-miR-24-2*	1	0	1
hsa-miR-26b*	1	0	1
hsa-miR-296-5p	1	0	1
hsa-miR-29b-2*	1	0	1
hsa-miR-30c-1*	1	0	1
hsa-miR-338-5p	0	1	1
hsa-miR-33a	1	0	1
hsa-miR-342-5p	0	1	1
hsa-miR-451	1	0	1
hsa-miR-499-5p	1	0	1
hsa-miR-524-5p	1	0	1
hsa-miR-545	1	0	1
hsa-miR-556-3p	1	0	1
hsa-miR-570	0	1	1
hsa-miR-625	1	0	1
hsa-miR-629*	1	0	1
hsa-miR-641	0	1	1
hsa-miR-7-2*	1	0	1
hsa-miR-744*	0	1	1

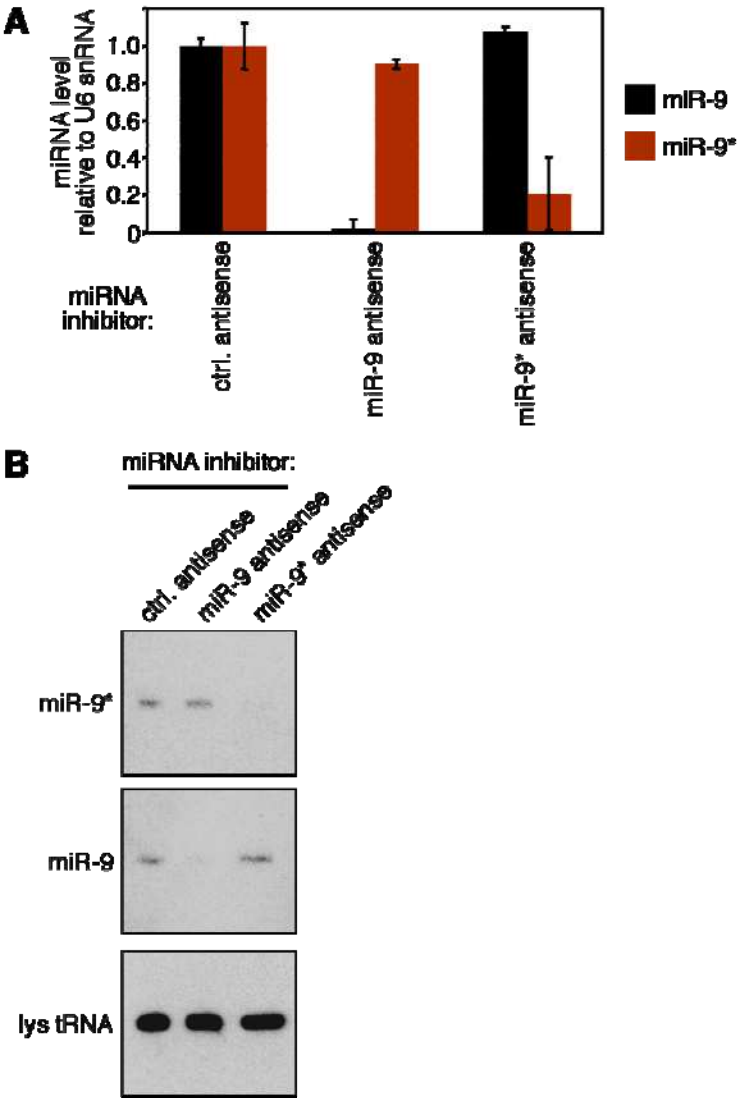

Schraivogel et al. Suppl. Figure 1

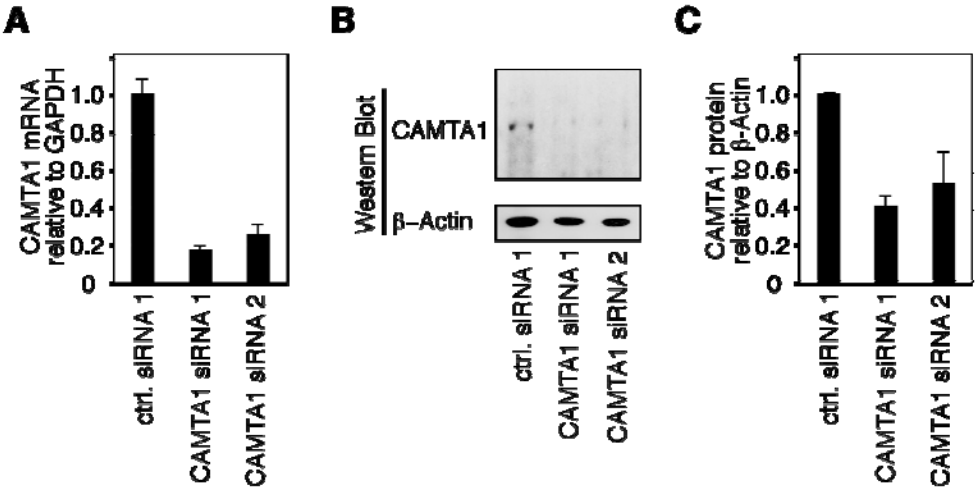

Schraivogel et al. Suppl. Figure 2

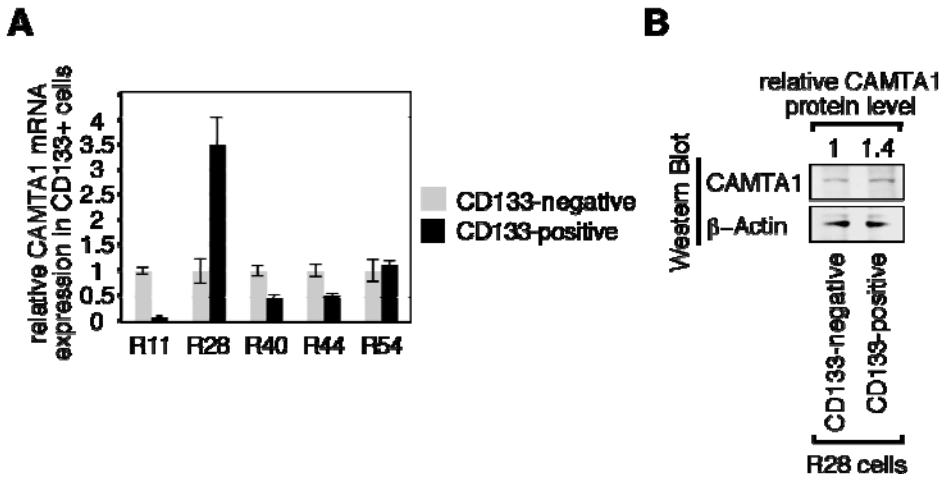

Schraivogel et al. Suppl. Figure 3